Dalton Transactions

ROYAL SOCIETY OF CHEMISTRY

PAPER

View Article Online
View Journal | View Issue

Cite this: *Dalton Trans.*, 2023, **52**, 2424

Rhodium and ruthenium complexes of methylene-bridged, *P*-stereogenic, unsymmetrical diphosphanes†‡

Javier Eusamio, [a,b] Yaiza M. Medina, [a,b] Javier C. Córdoba, [a] Anton Vidal-Ferran, [a,b,c] Daniel Sainz, [a,b] Albert Gutiérrez, [a,b] Mercè Font-Bardia[d] and Arnald Grabulosa *[a,b]

Received 15th December 2022,
Accepted 23rd January 2023

DOI: 10.1039/d2dt04026c

rsc.li/dalton

Enantiopure *P*-stereogenic methylphosphane-boranes (S_P)-P(BH$_3$)PhArMe (**ArMe**; Ar = 1-naphthyl (**NpMe**), and 2-biphenylyl (**BiphMe**)) have been used to prepare diphosphanes of the type ArPhPCH$_2$PR$_2$ (R = Ph, iPr or *t*Bu; **ArR**). The ligands have been reacted with [Rh(COD)$_2$]BF$_4$ to furnish the corresponding six monochelated [Rh(COD)(**ArR**)]BF$_4$ organometallic compounds (**RhArR**) or, depending on the reaction conditions, the bis(chelated) coordination compound [Rh(**BiphiPr**)$_2$]BF$_4$ as a mixture of *cis* and *trans* isomers. The crystal structure of *cis*-[Rh(**BiphiPr**)$_2$]BF$_4$ was obtained. The coordination of the **BiphR** with [RuCl(μ-Cl)(η^6-*p*-cymene)$_2$]$_2$ under different conditions produced cationic chelated complexes of the type [RuCl(η^6-*p*-cymene)(κ^2-**BiphR**)]PF$_6$ (**RuBiphR**) and the neutral monocoordinated complex [RuCl$_2$(η^6-*p*-cymene)(κ^1-**BiphPh**)] (**RuBiphPh'**) with the uncoordinated *P*-stereogenic moiety. The Rh(I) complexes were used in the catalytic hydrogenation of functionalized olefins and the Ru(II) complexes were tested in the transfer hydrogenation of acetophenone. Both precursors displayed good activities with moderate enantioselectivities.

Introduction

Throughout the history of organometallic homogeneous catalysis, phosphorus has been and remains the most important donor group in ancillary ligands of catalytic precursors, due to its ability to coordinate to most of the catalytically more capable metals.[1] Among the many phosphorus-based ligands that have been synthesized, diphosphanes are still the most popular, especially in enantioselective catalysis.[2,3] The relatively high inversion energy of phosphorus allows for the enantioselective preparation of *P*-stereogenic ligands,[4,5] which have been very successful in several enantioselective reactions. These *P*-stereogenic diphosphanes shone especially bright in the early days of asymmetric catalysis specifically in enantioselective hydrogenation,[6–9] to the point that one of the awardees of the 2001 Nobel Prize in Chemistry was William S. Knowles[10] for his research on the synthesis of L-DOPA —a drug used to treat Parkinson's disease— by enantioselective hydrogenation using the DIPAMP ligand, a *P*-stereogenic diphosphane.

After a long period with low activity, many more successful *P*-stereogenic diphosphanes have been developed,[5,11–15] affording excellent catalytic results. Some of the most successful have been those with a single atom linker between the two phosphorus atoms,[16] like the MiniPHOS family,[17,18] TriChickenFootPHOS (TCPF),[19] or MaxPHOS.[20–22] These short-bridged ligands (Fig. 1), despite their simple structures, have excelled in enantioselective hydrogenation.[23]

For these reasons, following our own research on *P*-stereogenic monophosphanes,[24–28] we recently reported an array of modular *P*-stereogenic diphosphanes with a methylene bridge and their Pd(II) complexes.[29] The ligands are rare examples of unsymmetrical (C_1-symmetric) diphosphanes, which have previously proved to be amongst the most efficient in metal-catalysed asymmetric hydrogenation.[17–19,23,30–34]

In the present work, we present two new ligands bearing a P(*t*Bu)$_2$ moiety on the non-stereogenic phosphorus, and the study of the coordination of this kind of ligands to Rh(I) and Ru(II), to further explore the coordinative variability they

[a]*Departament de Química Inorgànica i Orgànica, Secció de Química Inorgànica, Universitat de Barcelona, Martí i Franquès, 1-11, E-08028 Barcelona, Spain*
[b]*Institut de Nanociència i Nanotecnologia (IN2UB), Universitat de Barcelona, E-08028 Barcelona, Spain. E-mail: arnald.grabulosa@qi.ub.es*
[c]*Institució Catalana de Rercerca i Estudis Avançats (ICREA), Passeig Lluís Companys 23, E-08010 Barcelona, Spain*
[d]*Unitat de Difracció de Raigs X, Centres Científics i Tecnològics de la Universitat de Barcelona (CCiTUB), Solé i Sabarís 1-3, E-08028 Barcelona, Spain*

† In memoriam of Prof. Paul Kamer (1960–2020).

‡ Electronic supplementary information (ESI) available: NMR spectra of the new compounds. CCDC 2223261–2223263 for complexes **RhBiph*t*Bu**, **Rh(BiphiPr)$_2$** and **RuBiphiPr**. For ESI and crystallographic data in CIF or other electronic format see DOI: https://doi.org/10.1039/d2dt04026c

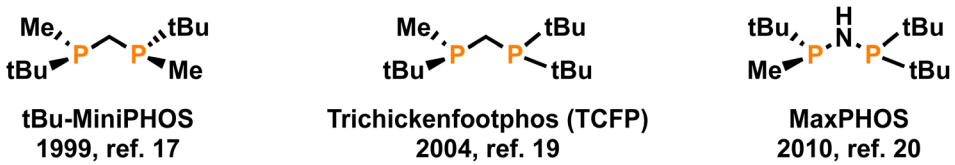

Fig. 1 Structures of MiniPHOS, TCFP and MaxPHOS.

display. In addition, catalytic results in the hydrogenation and transfer hydrogenation reactions are presented.

Results and discussion

Unsymmetrical diphosphanes

The methylene-bridged diphosphanes $ArPhP^1CH_2P^2R_2$ (**ArR**; Ar = 2-biphenylyl (Biph) and 1-naphthyl (Np); R = iPr, *t*Bu or Ph) contain an enantiopure *P*-stereogenic moiety (denoted as P^1) and a non-*P*-stereogenic moiety (denoted as P^2). The ligands were prepared from optically pure methylphosphane–boranes (**ArMe**) by deprotonation of the methyl group and phosphination of the resulting carbanion with the corresponding chlorophosphane[29] (Fig. 2). The diphosphanes could be conveniently stored as their bis(borane) adducts (**ArR·BH$_3$**), which can be easily deprotected when needed with morpholine.

Given the good results that several *P*-stereogenic diphosphanes containing the bis(*tert*-butyl)phosphino group have produced in enantioselective catalysis,[13,22] the same procedure was followed to prepare the protected diphosphane **Biph*t*Bu·BH$_3$** (Fig. 2). Unexpectedly, it was found that this compound could not be isolated, but the monoboronated adduct **Biph*t*Bu·2-BH$_3$** —with only the P^2 phosphorus protected— was instead obtained (Fig. 3), a compound that was found to be stable in air for a few days.

In the $^{31}P\{^1H\}$ NMR spectrum of the reaction mixture after workup, **Biph*t*Bu·2-BH$_3$** was observed as a broad singlet at δ_P = +45.1 ppm and a sharp doublet at −30.2 ppm ($J_{P^1-P^2}$ = 46.1 Hz), corresponding to P^2 and P^1 respectively. The formation of **Biph*t*Bu·BH$_3$** (with both phosphorus boronated) could only be observed by $^{31}P\{^1H\}$ NMR spectroscopy in solution in the presence of an excess of BH_3·THF as two broad signals at δ_P +50.3 and +26.3 ppm, corresponding to P^2 and P^1, respectively. After following the aqueous work-up as in the previously reported procedure,[29] the species **Biph*t*Bu·2-BH$_3$** was obtained, meaning that P^1 had suffered a spontaneous deboronation reaction. This result can be explained first by the reduced basicity of the diarylphosphane P^1 compared to the trialkylphosphane P^2 and, second, by the steric hindrance exerted by the

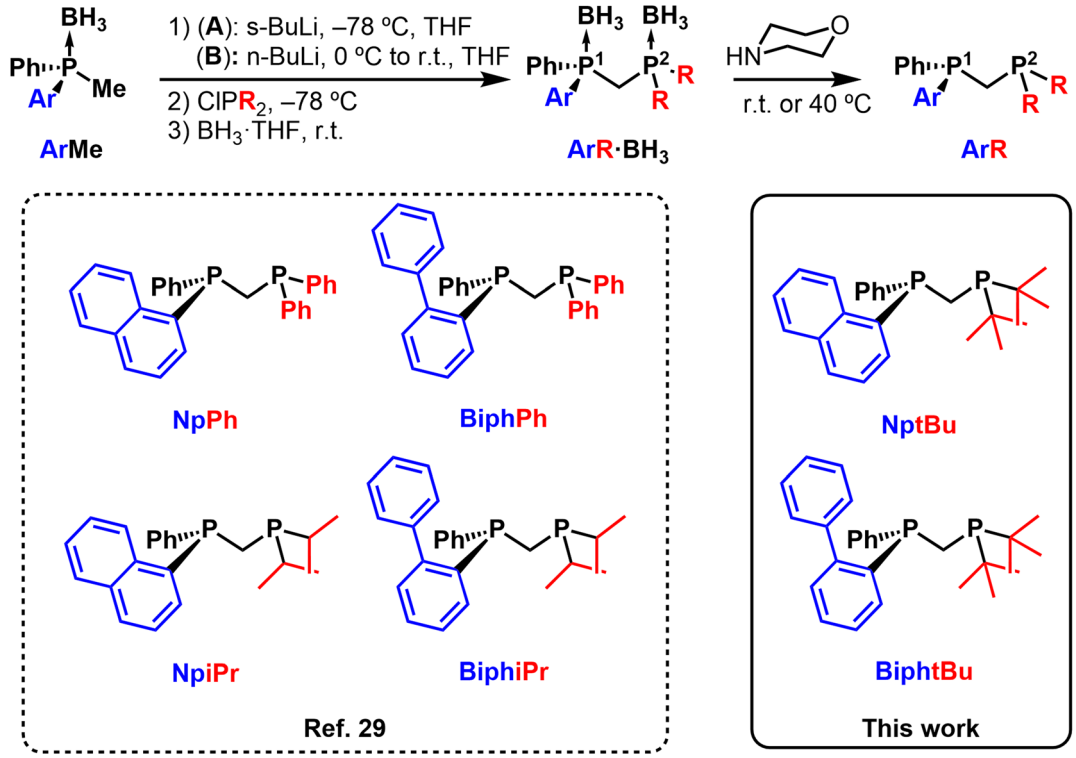

Fig. 2 Synthesis of the unsymmetrical diphosphanes. **Npt*Bu*** was synthesized by a variation of method **A**, and **Biph*t*Bu** with a variation of method **B**.

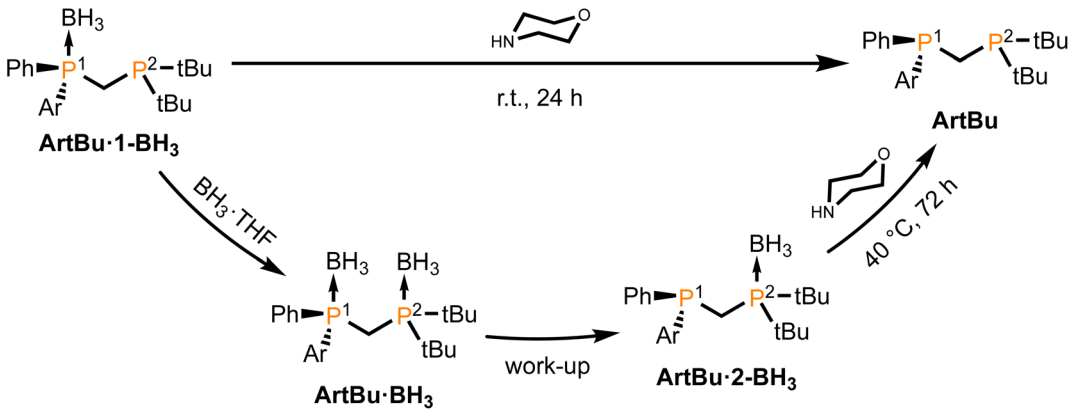

Fig. 3 Synthesis of **ArtBu** diphosphanes.

bis(*tert*-butyl)phosphane moiety of P^2, weakening the B–P^1 bond. It has to be noted that these two factors are necessary for the spontaneous cleavage of the B–P bond, since borane adducts of both alkyl,[18,19] and aryldiphosphanes[29,35,36] with a methylene bridge are known to be perfectly stable compounds.

The deprotection of **Biph*t*Bu·2-BH$_3$** with morpholine[29,37] was found to be very slow, requiring 72 h at 40 °C (Fig. 3). The synthesis was therefore adapted to furnish **Biph*t*Bu** in a one-pot procedure, treating without isolation the intermediate compound **Biph*t*Bu·1-BH$_3$** —with only P^1 protected— with morpholine at room temperature for 24 h (Fig. 3). Following this same procedure, the ligand **Np*t*Bu** was also synthesized and fully characterized.

The $^{31}P\{^1H\}$ NMR spectra of ligands **Biph*t*Bu** (δ_{P^1} = −24.1 ppm, δ_{P^2} = +15.3 ppm; $J_{P^1-P^2}$ = 127.7 Hz) and **Np*t*Bu** (δ_{P^1} = −28.1 ppm, δ_{P^2} = +13.8 ppm; $J_{P^1-P^2}$ = 143.8 Hz) consist of two doublets while the hydrogen atoms of the *tert*-butyl groups appear in the ^1H NMR spectra as two sharp doublets (J_{H-P^2} = 10.8 Hz) at around 0.8 ppm, in accordance with other methylene-bridged diphosphanes.[29,38,39]

Rhodium complexes

Initially, we focused on obtaining the rhodium(I) complexes with the general formulae [Rh(**ArR**)(COD)]BF_4 (**RhArR**), which are typical hydrogenation catalytic precursors,[23,40] starting from the rhodium precursor [Rh(COD)$_2$]BF_4 (Fig. 4).

However, upon adding one equivalent of [Rh(COD)$_2$]BF_4 to a solution of one equivalent of the deprotected diphosphane, a complex mixture of species was observed according to $^{31}P\{^1H\}$ NMR, after a standard work-up in air. At lower field (50–20 ppm) some peaks probably corresponding to the oxidized diphosphanes[39,41,42] could be identified while at higher field (with a chemical shift between 0 and −40 ppm), where the signals of the Rh–P complexes tend to appear,[19,43–49] more than one species was observed. From the presence of oxidized diphosphanes, it was deduced that the complexes were air-sensitive and tended to decompose when exposed to air, an uncommon feature for compounds with this structure, which are often stable.[19] However, some hints in the literature suggest a certain lability of the ligands.[50]

The repetition of the syntheses and work-up under strictly inert atmosphere solved the oxidation issues, but a mixture of species was still observed at higher field in $^{31}P\{^1H\}$ NMR spectra. From the great variety of coordination possibilities that the ligands had shown when coordinated to Pd(II),[29] it was assumed that more than one metal complex could be formed. In the literature, some examples of bischelated complexes were found for short-bridged ligands so we wondered whether mixtures of mono- and bischelated complexes could be formed (Fig. 5).[17,32,33]

To favour the formation of the mono(chelated) structure, the order of the complexation was altered, adding a solution of the diphosphane to a solution of the rhodium precursor in a

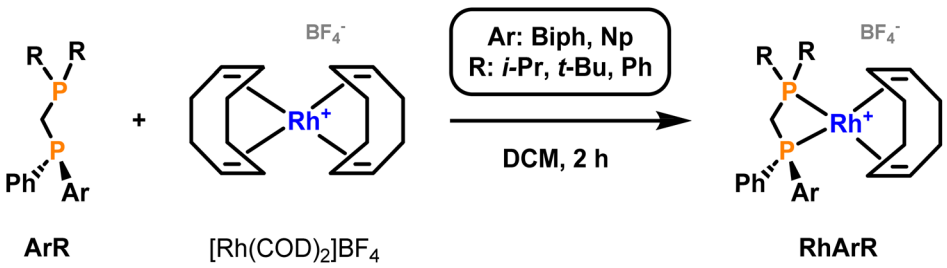

Fig. 4 Synthesis of the **RhArR** complexes.

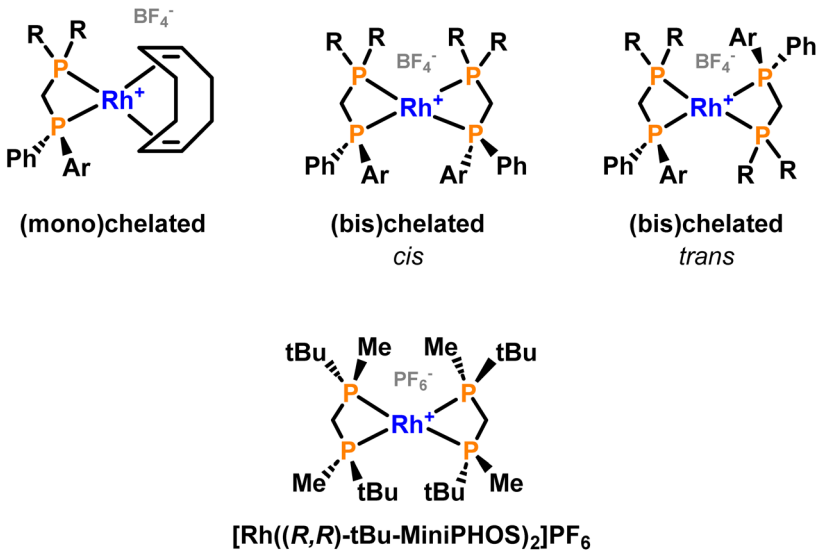

Fig. 5 General structure of the mono(chelated) and bis(chelated) complexes (top) and an example of a reported bis(chelated) complex with a methylene-bridged diphosphorus ligand (bottom).[17]

dropwise manner under vigorous stirring,[19,32,33,50,51] to ensure a low local concentration of the ligand and thus avoid the formation of the bis(chelated) complexes. This new procedure afforded the pure mono(chelated) structures after recrystallisation under inert atmosphere. The complexes were found to be indefinitely stable if kept under nitrogen at low temperature. In Fig. 6 the $^{31}P\{^{1}H\}$ NMR spectra of the complexes are displayed and the values of the chemical shifts and coupling constants are given in Table 1.

Each compound features two doublets of doublets, each one corresponding to one of the phosphorus atoms, coupled to the other one and to the rhodium nucleus. As it can be seen, the chemical shift for the *P*-stereogenic phosphorus (P^1) ranges between −40 and −33 ppm. The shift of the non-*P*-

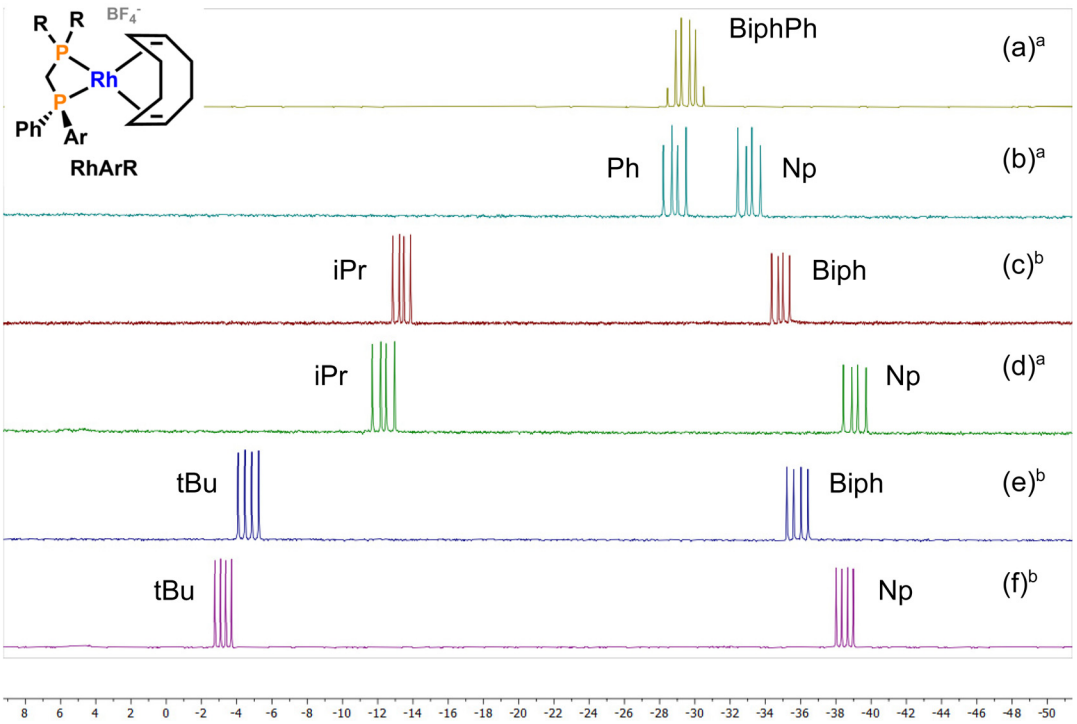

Fig. 6 $^{31}P\{^{1}H\}$ NMR (CD_2Cl_2) spectra of the mono(chelated) Rh complexes. (a) **RhBiphPh**, (b) **RhNpPh**, (c) **RhBiphiPr**, (d) **RhNpiPr**, (e) **RhBiphtBu**, (f) **RhNptBu**. [a] At 162 MHz. [b] At 202 MHz.

Table 1 $^{31}P\{^1H\}$ NMR (CD_2Cl_2) shifts (ppm) and coupling constants (Hz) for the rhodium complexes **RhArR**

Complex	δ_{P^1}	δ_{P^2}	$^2J_{P^1-P^2}$	$^1J_{P^1-Rh}$	$^1J_{P^2-Rh}$
RhBiphiPr[a]	−34.9	−13.4	76.1	129.4	126.9
RhBiph*t*Bu[a]	−35.8	−4.7	63.1	130.6	125.4
RhBiphPh[b,c]	−29.8	−29.1	75.7	130.6	126.6
RhNpiPr[b]	−39.1	−12.3	77.4	131.7	126.7
RhNp*t*Bu[a]	−38.3	−2.9	63.9	132.7	125.1
RhNpPh[b]	−33.1	−28.9	78.0	130.1	130.2

[a] 202 MHz. [b] 162 MHz. [c] Values obtained using the software package Spinworks.[52]

stereogenic phosphorus (P^2) is defined by its substituents: *ca.* −30 ppm for PPh_2, −12 for $PiPr_2$ and −3 ppm for $PtBu_2$. This order is given by a combination of acidity and bulkiness of the substituents, influence of which on $^{31}P\{^1H\}$ NMR shifts has been well studied and match with comparable complexes containing diphosphanes with the PPh_2, $PiPr_2$ and $PtBu_2$ groups.[19,43,46–49,51,53]

In the case of **RhBiphPh**, the two phosphorus are so similar that they appear almost overlapped, appearing as a multiplet in the NMR spectrum due to a rather strong *roofing effect* on the peaks while in the case of complexes **RhBiph*t*Bu** and **RhNp*t*Bu** the separation between the shifts of the phosphorus is more than 30 ppm and no *roofing effect* is observed whatsoever.

Obtaining single crystals of the complexes for X-ray diffraction measurements was found to be difficult, due to their tendency to form oily substances and their air sensitivity. Nonetheless, after many attempts we managed to obtain a single crystal of complex **RhBiph*t*Bu** (Fig. 7) by vapor diffusion of hexane into a concentrated solution of the complex in tetrahydrofuran.

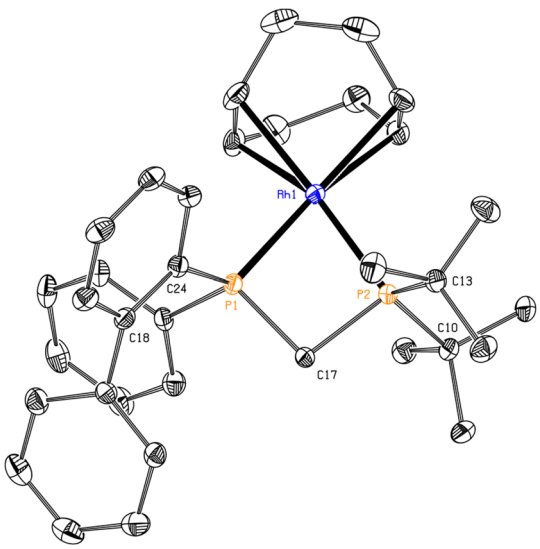

Fig. 7 ORTEP plot of **RhBiph*t*Bu** with ellipsoids drawn at 50% probability level. Hydrogen atoms and the tetrafluoroborate anion have been omitted for clarity. Selected distances (Å) and angles (°): Rh1–P1 2.2861 (7), Rh1–P2 2.3356(7), P1–C17 1.837(3), P2–C17 1.857(3), P1–Rh1–P2 72.35(2).

As it can be seen, the bond distance between the rhodium atom and the *P*-stereogenic phosphorus (P^1) is shorter than that of its non-*P*-stereogenic counterpart (P^2), probably accounting for the bulkiness of the $PtBu_2$ moiety. The bite angle, 72.35(2)°, differs considerably from the ideal 90° that corresponds to square planar structures, but its value is within the range found for other Rh(I) complexes with diphosphane ligands with single-atom linkers.[19,21,50,54–56]

After having obtained the mono(chelated) complexes we focused on obtaining a pure bis(chelated) complex. To this end, a solution of slightly less than two equivalents of ligand **BiphiPr** was treated with one equivalent of $[Rh(COD)]_2BF_4$ in dichloromethane. The apparently simple reaction posed a greater challenge than expected since the formation of some amount of mono(chelated) complex was observed (Fig. 8a and b), even when working at a stoichiometric ratio of ligand/Rh precursor of 2 : 1. This has been previously observed by Vidal-Ferran and coworkers in Rh(I) complexes with narrow bite-angle chiral phosphane–phosphite ligands.[32,33] Finally, adjusting the reaction conditions, it was possible to obtain the bis(chelated) complex **Rh(BiphiPr)$_2$** containing only a small amount (~1–2%) of **RhBiphiPr**. High-resolution ESI-MS analysis revealed the presence of the M^+ cation at m/z = 887.2698 (requires 887.2701), while the $^{31}P\{^1H\}$ NMR spectrum showed a complex spectrum (Fig. 8c).

The compound features a complex $^{31}P\{^1H\}$ NMR spectrum (Fig. 8c) comprising six highly symmetric multiplets with chemical shifts between 0 and −28 ppm. The high-field signals in the $^{31}P\{^1H\}$ NMR spectrum are in the range expected for methylene-bridged diphosphanes (for dppm[43] and dcypm[48] δ_P = −23.3 and −16.9 ppm, respectively) and the complexity of is not unexpected since a mixture of the *cis* and *trans* isomers (Fig. 5) could be present and both constitute second order AMM′XX′ spin systems[32,57] (M and M′ represent P^2, X and X′ P^1 and A, Rh). To confirm that an isomeric mixture was present, a bidimensional homonuclear COSY $^{31}P\{^1H\}$–$^{31}P\{^1H\}$ NMR experiment (Fig. 9) and also a HMBC ^1H–$^{31}P\{^1H\}$ (see ESI‡) were carried out.

The COSY spectrum clearly shows a correlation between the two central multiplets and the four external multiplets, but not between these two groups of signals. Therefore, it was deduced that the complex was present as a mixture of *cis*- and *trans*-isomers in an approximate 1 : 1.4 ratio.

Several attempts to separate the isomers by crystallization failed, but changes in the relative integrations of the two mentioned groups of signals in the recrystallized solids and the mother liquors were observed. This confirmed that two species were present and indicating that their separation could be possible. Luckily, it was possible to grow single crystals of the complex (Fig. 10), which corresponded to ***cis*-Rh(BiphiPr)$_2$**. The $^{31}P\{^1H\}$ NMR spectrum of a crystal after its dissolution in $CDCl_3$ was recorded (Fig. 8d). From the figure it can be seen that the multiplets between −24 and −28 ppm and between 0 and −4 ppm correspond to ***cis*-Rh(BiphiPr)$_2$**. The structure of

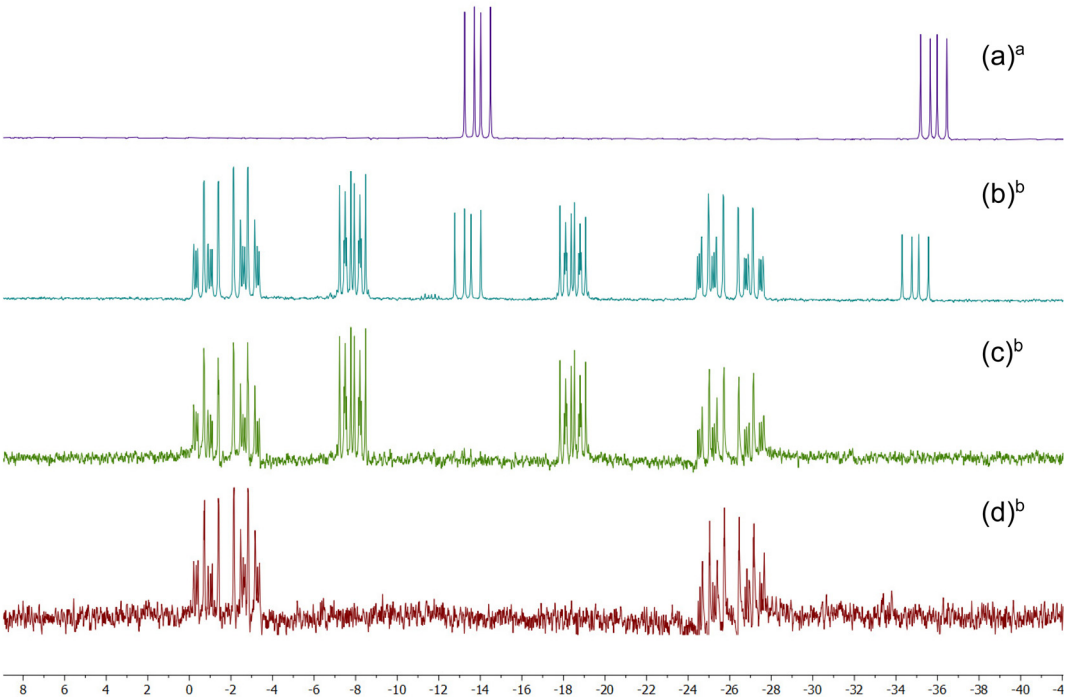

Fig. 8 $^{31}P\{^{1}H\}$ NMR spectra (CD_2Cl_2) of the mono- and bis(chelated) complexes. (a) Pure **RhBiphiPr**; (b) crude mixture of **RhBiphiPr** and **Rh(BiphiPr)$_2$**; (c) ~99% pure **Rh(BiphiPr)$_2$** as a mixture of *cis*- and *trans* isomers; (d) pure ***cis*-Rh(BiphiPr)$_2$** from a monocrystal. [a] At 202 MHz. [b] At 162 MHz.

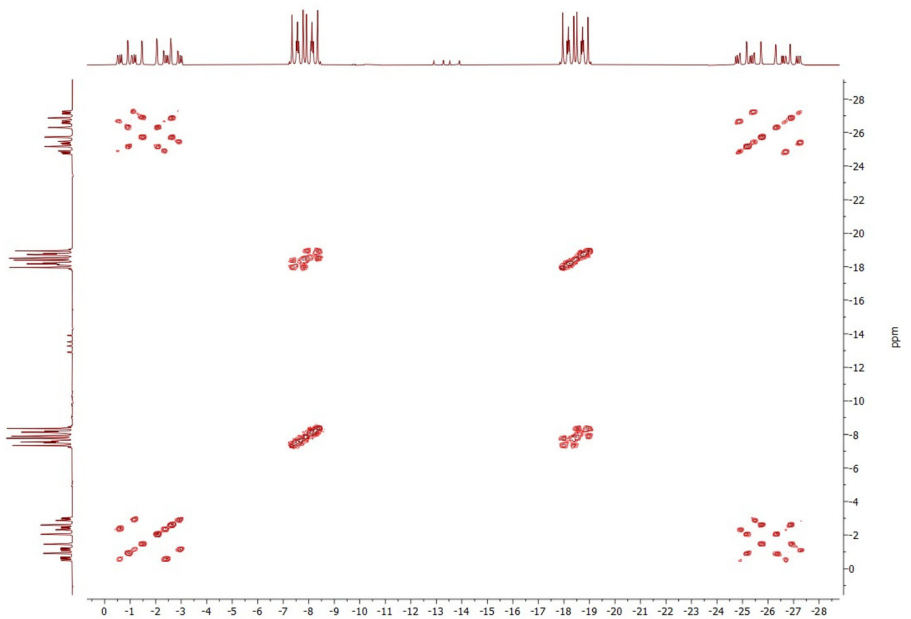

Fig. 9 COSY $^{31}P\{^{1}H\}$–$^{31}P\{^{1}H\}$ NMR spectrum (202 MHz, CD_2Cl_2) of **Rh(BiphiPr)$_2$**.

***cis*-Rh(BiphiPr)$_2$**, obtained by X-ray diffraction, is to our knowledge the first reported example of a Rh(I) bis(chelated) complex with an unsymmetrical diphosphane (Fig. 10).

Interestingly, the isomer that crystallized was ***cis*-Rh(BiphiPr)$_2$**, exactly the same that had been observed with Pd (II).[29] As both isomers are formed in approximately equal ratio, it is reasonable to think that the *cis* isomer is more insoluble and easier to precipitate.

In the crystal structure, the bite angle matches that of the mono(chelated) structure with the same ligand and of other

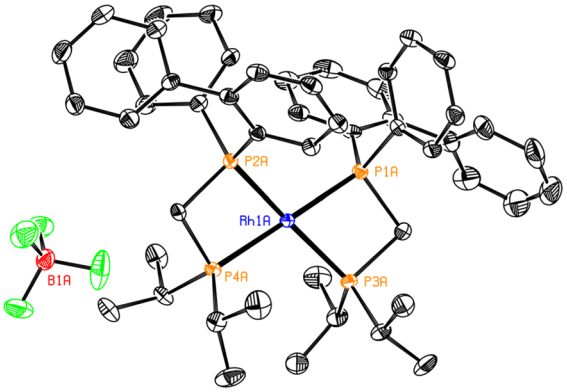

Fig. 10 ORTEP plot of the crystal structure of ***cis*-Rh(BiphiPr)$_2$** with ellipsoids drawn at 50% probability level. Hydrogen atoms have been omitted for clarity. Selected distances (Å) and angles (°): P1A–Rh1A 2.295(1), P2A–Rh1A 2.328(1), P3A–Rh1A 2.292(1), P4A–Rh1A 2.297(1), P1A–Rh1A–P3A 72.60(4), P2A–Rh1A–P4A 72.72(4), P1A–P2A–P3A–P4A −1.40(3).

reported bis(chelated) complexes with similar ligands.[17,58] The near-zero torsion angle indicates that the Rh centre adopts a nearly perfect square-planar configuration, even though the bite angle differs greatly from the ideal 90°.

Despite many attempts, it was not possible to obtain, in a synthetically useful way, the pure isomers although the obtention of a crystal of ***cis*-Rh(BiphiPr)$_2$** shows that it should be possible by simple recrystallisation.

Ruthenium complexes

After the study of the coordination chemistry of the ligands in the square-planar environments of d^8 palladium(II)[29] and rhodium(I) we decided to study their behaviour with the well-known ruthenium(II)-*p*-cymene unit, to form octahedral, d^6 Ru(II) complexes. Two ligands with a 2-biphenylyl moiety (**BiphiPr** and **BiphPh**) were chosen because it seems to lead to more stable and crystalline complexes.

Following previous studies,[59] 2 eq. of the **BiphR** ligand were added to a dichloromethane solution of [RuCl(μ-Cl)(η^6-*p*-cymene)]$_2$ containing 5 equivalents of NH_4PF_6 in order to form the cationic complexes [RuCl(η^6-*p*-cymene)(**BiphR**)]PF_6, (**RuBiphR**, Fig. 11, top). However, similarly to what had been observed with Rh(I) and Pd(II),[29] the reactions yielded several types of complexes, shown in Fig. 11 (bottom). It has to be noted that the complexes tend to form oils that had to be triturated with diethyl ether or pentane to give the final compounds as orange or reddish solids, a fact that has been mentioned in the literature for similar complexes.[60]

Interestingly, the coordination behaviour is determined by the substituents of the non-*P*-stereogenic atom, P^2. The ligand **BiphiPr**, with the relatively bulky iPr groups preferentially forms the chelated structures,[61] regardless of the addition of PF_6 as a counterion or not. Hence, **RuBiphiPr** was isolated with the standard procedure (Fig. 11, top) and when NH_4PF_6 was not added, **RuBiphiPrCl** was obtained instead, with chloride as a counterion.

For the two complexes, very clean ESI-MS spectra with a single peak at m/z = 663.2 were obtained, corresponding to the parent [RuCl(*p*-cymene)(**BiphiPr**)]$^+$ cation. In the $^{31}P\{^1H\}$ spectra NMR, both complexes featured two pairs of doublets at δ_P of approximately +21 and 0 ppm with a coupling constant of *ca.* 91 Hz. The chemical shifts can be compared to those of the related complexes with the simple κ^2-coordinated ligand dppm, reported to occur at δ_P of +2.7 (PF_6),[60] +0.4 ppm (Cl)[62] and similarly for other anions[63,64] in accordance with the expected upfield shift due to the ring effect of a four-membered metallacycle.[60,65–67] In addition, the spectrum of complex **RuBiphiPr** contains the diagnostic septet centred at −142.0 ppm of the hexafluorophosphate anion. It is interesting

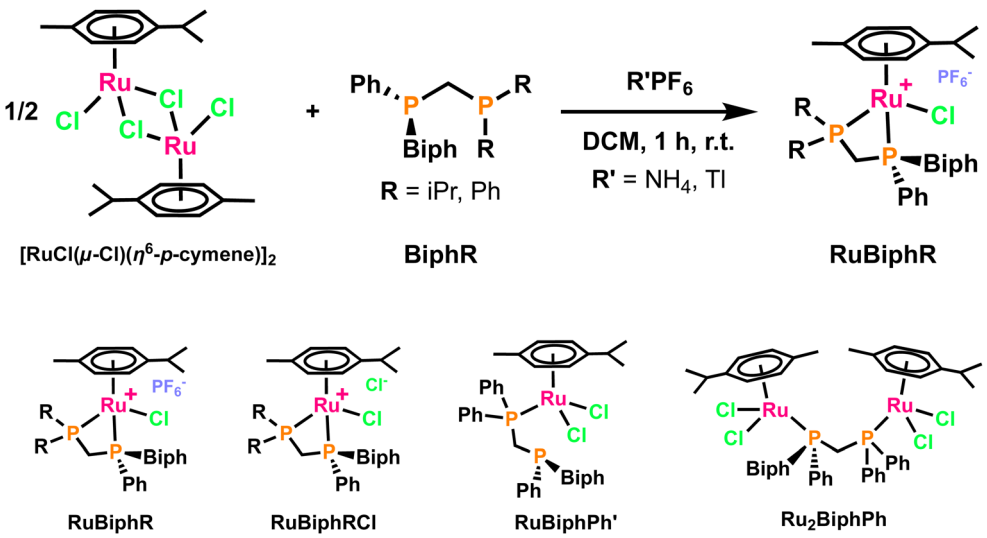

Fig. 11 Top: reaction scheme for the complexation of the ligands to Ru(II) complexes. Bottom: structures of the different complexes.

to note that a single set of signals was observed in $^{31}P\{^{1}H\}$, $^{13}C\{^{1}H\}$ and ^{1}H spectra, suggesting that the complexes are present as single species in solution despite the fact that the ruthenium atom becomes a stereogenic centre and two configurations are possible. The rigidity of the rings probably accounts for this fact, as it happened with the short-bridge ligand MaxPHOS.[59]

In the case of the ligand **BiphPh**, the standard conditions (Fig. 11, top) did not provide the expected chelated complex **RuBiphPh**, but the monocoordinated complex **RuBiphPh′**, with the **BiphPh** ligands coordinated in a κ^1 fashion (Fig. 11, bottom). Obviously, the very same complex was obtained if NH_4PF_6 was not added. There is only one related complex described in the literature, bearing the dppm ligand coordinated in κ^1 fashion.[68–70]

The identity of **RuBiphPh′** was confirmed by the ESI-MS spectrum, with the base peak at m/z = 767.1 corresponding to the $[M + H]^+$ ion. Interestingly, a minor peak at m/z = 731.1 can also be detected, which can be assigned to the $[M - Cl]^+$ cation, in which the ligand presumably acts as bidentate, most probably formed during the ionization process in the mass spectrometer chamber. The $^{31}P\{^{1}H\}$ showed the absence of the hexafluorophosphate anion and the presence of two sharp doublets at δ_P of +20.9 and −36.9 ppm (in $CDCl_3$), with a coupling constant of 31.0 Hz. These values can be conveniently compared to those reported for the related complex with a κ^1-coordinated dppm (δ_P = +26.1, −27.6 ppm; J_{PP} = 31.8 Hz)[68,69] and for the free **BiphPh** (δ_{P^1} = −29.7 ppm, δ_{P^2} = −22.6 ppm; $J_{P^1-P^2}$ = 126.8 Hz). This comparison reveals that the **BiphPh** ligand is coordinated to the Ru(II) atom by the non-*P*-stereogenic phosphorus P^2, probably due to steric effects, preventing the coordination of the more crowded *P*-stereogenic atom P^1 bearing the 2-biphenylyl substituent. Interestingly, when the $^{31}P\{^{1}H\}$ was recorded in CD_3OD the spectrum looked completely different (δ_P = +6.9, −2.4 ppm; $J_{P^1-P^2}$ = 99.5 Hz) because it corresponded to the chelated complex **RuBiphPhCl**, highlighting the subtle effects that govern the chelation of the methylene-bridged diphosphanes. A similar solvent effect was observed by Dyson and coworkers[71] for dppm. After performing kinetic studies, they concluded that methanol favours ring-closing due to hydrogen bond formation with the chloride ligands, helping in their activation.

The synthesis and isolation of **RuBiphPh** was finally achieved using $TlPF_6$ instead of NH_4PF_6, the former being a much stronger halide scavenger.[28,72,73] This reaction was effective if the starting reagents were either $[RuCl(\mu\text{-}Cl)(\eta^6\text{-}p\text{-cymene})]_2$ and the free **BiphPh** ligand, or the monodentate **RuBiphPh′** complex, yielding the cationic complex after filtration of thallium chloride. The ESI-MS spectrum featured the expected peak centred at m/z = 731.1, corresponding to the organometallic cation. The $^{31}P\{^{1}H\}$ NMR spectrum confirmed the identity of **RuBiphPh**, showing the expected coupled pair of doublets (δ_{P^1} = −2.4 ppm, δ_{P^2} = +6.9, $J_{P^1-P^2}$ = 99.6 Hz) apart from the septet of the hexafluorophosphate anion. The chemical shift values are very similar to those of the analogous complex with dppm.[60] It is interesting to note that the $^2J_{P^1-P^2}$ in the chelated complexes is around 100 Hz but only 30 Hz in the complexes with the monocoordinated ligands.

Finally, **BiphPh** was treated with an excess of $[RuCl(\mu\text{-}Cl)(\eta^6\text{-}p\text{-cymene})]_2$ in order to obtain the bimetallic complex **Ru_2BiphPh**, as described in the literature a long time ago with dppm by Atwood, Dixneuf, Bonnet and coworkers[74,75] and by Lahuerta and coworkers[76] and much more recently by Blom and coworkers[77] using η^6-benzene instead of η^6-*p*-cymene. However, after a few attempts including heating a dichloromethane solution of the Ru dimer and the **BiphPh** ligand to reflux for several hours,[77] the desired complex was not formed, and only **RuBiphPh′**, impurified with **RuBiphPhCl**, free *p*-cymene and other species due to decomposition[78] was obtained. This unsuccessful synthesis shows that the steric crowding of the **BiphPh** ligand makes it rather different compared to dppm, despite having very similar electronic characteristics.

The crystal structure of **RuBiphiPr** was obtained (Fig. 12) after slow diffusion of hexane onto a saturated solution of the complex in dichloromethane. It appears that the complexes bearing the **BiphiPr** ligand are more prone to crystallize, since it is the only ligand for which it has been possible to elucidate at least one crystal structure for all the metals to which it has been coordinated (Pd,[29] Rh, and Ru), and also the only one to have an elucidated crystal structure in its boronated form.[29]

As it can be seen in the figure, the complex forms a pseudo-tetrahedral structure, widely known as *three-legged piano-stool*, typical for this kind of complexes. The distance Ru-centroid

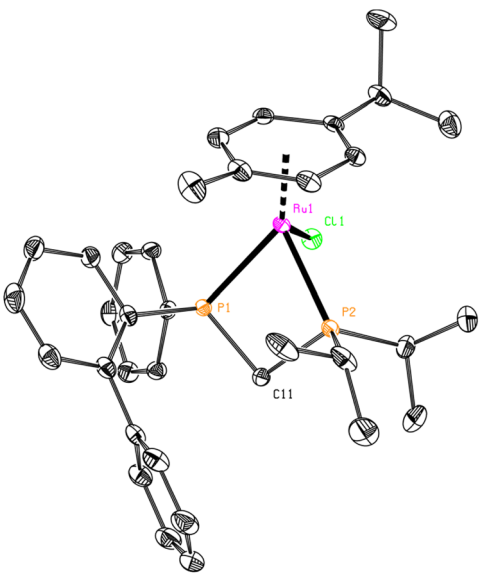

Fig. 12 ORTEP plot of the crystal structure of **RuBiphiPr** with ellipsoids drawn at 50% probability level. Hydrogen atoms and the hexafluorophosphate anion have been omitted for clarity. Selected distances (Å) and angles (°): Ru1–centroid 1.760, Ru1–Cl1 2.3825(6), Ru1–P1 2.3492(5), Ru1–P2 2.3399(5), P1–C11 1.8341(19), P2–C11 1.8369(19); P1–Ru1–P2 70.997(17), Cl1–Ru1–P1 83.886(17), Cl1–Ru1–P2 85.467(18), centroid–Ru1–Cl1 122.51, centroid–Ru1–P1 139.43, centroid–Ru1–P2 134.66, P1–C11–P2 95.76(9).

(1.760 Å) is similar to other [RuCl(η⁶-*p*-cymene)(κ²-diphosphane)]⁺ complexes.[60] The bite angle of the diphosphane in the complex (71.00(2)°) is much smaller than that observed with the same ligand in a Pd(II) complex (74.266(18)°)[29] and in the Rh complex **Rh(BiphiPr)$_2$** (72.60(4)° and 72.72(4)°) discussed before, but very similar to the bite angle of dppm[62,63,79] and a related ligand[66] in the few crystal structures reported for Ru(II) compounds containing the cation [RuCl(η⁶-*p*-cymene)(κ²-dppm)]. The smaller bite angle with Ru(II) is probably due to the octahedral coordination geometry enforced by a d^6 metal, that allows the methylene-bridged diphosphane to reach its "natural" bite angle of 72°.[16,80,81] The absolute configuration of the Ru centre is S_{Ru} according to the priority sequence η⁶-*p*-cymene > Cl > P(Biph)Ph > P(iPr)$_2$ and the Cahn–Ingold–Prelog Rules.[82–84]

Table 2 Asymmetric hydrogenation results with methanol

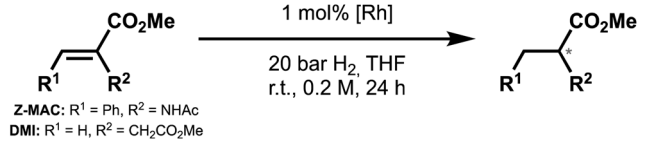

Entry	Catalyst	Substrate	Conversion (%)	ee (%)
1	**RhBiphiPr**	*Z*-MAC	>99	16 (*R*)
2		DMI	>99	29 (S)
3	**RhBiph*t*Bu**	*Z*-MAC	61	*rac*
4		DMI	>99	*rac*
5	**RhBiphPh**	*Z*-MAC	>99	24 (*R*)
6		DMI	>99	6 (*S*)
7	**RhNpiPr**	*Z*-MAC	>99	29 (*R*)
8		DMI	>99	23 (*S*)
9	**RhNp*t*Bu**	*Z*-MAC	>99	50 (*R*)
10		DMI	>99	9 (*S*)
11	**RhNpPh**	*Z*-MAC	>99	16 (*R*)
12		DMI	>99	*rac*
13	**Rh(BiphiPr)$_2$**	*Z*-MAC	12	*rac*
14		DMI	59	*rac*

Rh-catalysed hydrogenation

The rhodium complexes described in a previous section were explored as catalytic precursors in the reaction of asymmetric hydrogenation.[23] Two typically used benchmark substrates, *Z*-MAC ((*Z*)-methyl α-acetamido cinnamate) and DMI (dimethyl itaconate) were subjected to hydrogenation using 1% of Rh precursor at 20 bar of hydrogen pressure (Table 2).

The precursors are active in the reaction, leading to full conversions except for the hydrogenation of *Z*-MAC with **RhBiphiPr** (entry 3) and the two catalytic runs with **Rh(BiphiPr)$_2$** (entries 13 and 14). The lower activity of these precursors can be understood by the steric hindrance of the ligand and by the fact that the latter complex does not contain a labile ligand. Indeed, Imamoto and coworkers found a similar behaviour when studying their mono- and bis(chelated) complexes with MiniPHOS in hydrogenation.[17,18] Regarding the enantioselectivities, they are moderate, without a clear pattern and reaching a maximum value of 50% (entry 9), with *Z*-MAC usually giving slightly better enantioselectivities, as it is usually found.[5,23,40] As expected, the sense of enantioinduction is the same.[85]

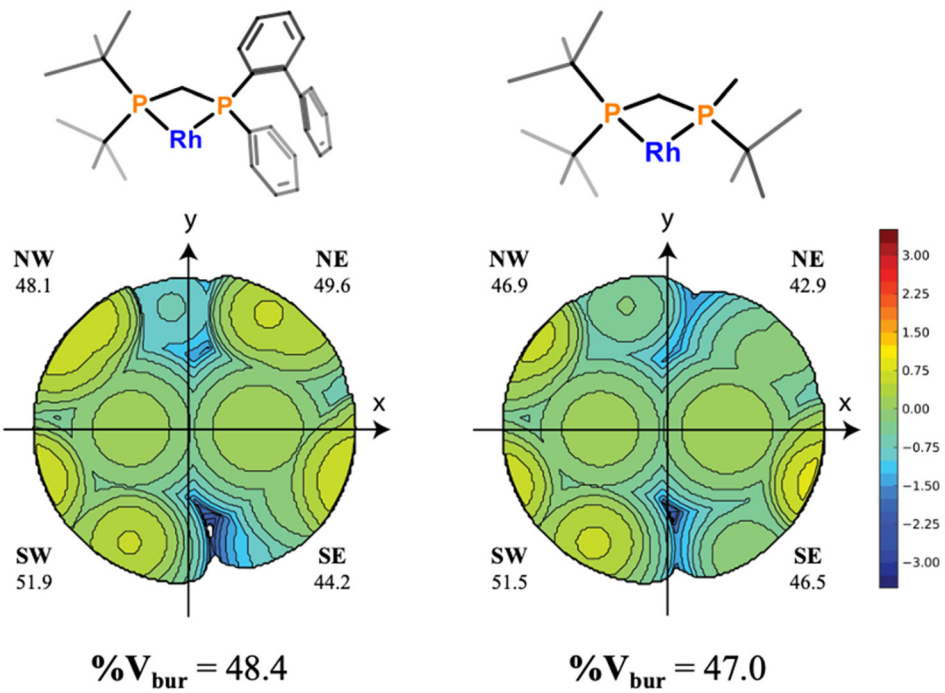

Fig. 13 Topographic steric maps and %V_{bur} values (for each quadrant and average value) of **Biph*t*Bu** using the crystal structure of **RhBiph*t*Bu** (Fig. 7) (left) and TCFP using the crystal structure of [Rh(cod)$_2$TCFP]BF$_4$ [19] (right).

The moderate enantioselectivities obtained with the ligands of this manuscript and the availability of the crystal structures of **RhBiph*t*Bu** (Fig. 7) and the analogous complex with the related ligand TriChickenFootPhos (TCFP, a highly enantioselective ligand in enantioselective hydrogenation),[86] reported by Hoge and coworkers,[19] prompted us to evaluate the steric properties of these two ligands by calculation of the percent buried volume (%V_{bur}) parameter[87] and the topographic steric maps using the SambVca 2.1 web application[88–90] (Fig. 13).

The averaged %V_{bur} values of the two ligands is indeed very similar with **Biph*t*Bu** being slightly bulkier than TCFP. The spatial distribution of this bulkiness, however is rather different for the two ligands because the normalised %V_{bur}(NW + SW) : %V_{bur}(NE + SE) ratios are 100 : 94 and 100 : 91 for **Biph*t*Bu** and TCFP respectively. This means that in TCFP the steric differentiation between the two phosphane moieties (*i.e.* between the eastern and western halves in the topographic maps of Fig. 13) is more pronounced than for **Biph*t*Bu**. In addition, the NE quadrant is more sterically unhindered in TCFP than the comparable SE quadrant for **Biph*t*Bu**.[91] It can be concluded that the phenyl/2-biphenylyl substituents of P^1 are probably not distinct enough and hence the introduction at this phosphorus of a bulkier aromatic group instead of 2-biphenylyl could be a strategy to explore future generations of the ligands.[92]

Ru-catalysed transfer hydrogenation

Ruthenium–arene complexes with *P*-stereogenic monophosphanes have been used by us[26–28,93,94] and others[95] in the catalytic reduction of ketones under transfer hydrogenation reactions. Following these studies, ruthenium complexes **RuBiphiPr**, **RuBiphiPrCl** and **RuBiphPh′** were studied as catalytic precursors, at 1% catalyst loading, in the transfer hydrogenation of acetophenone in refluxing isopropanol in the presence of base (Fig. 14).

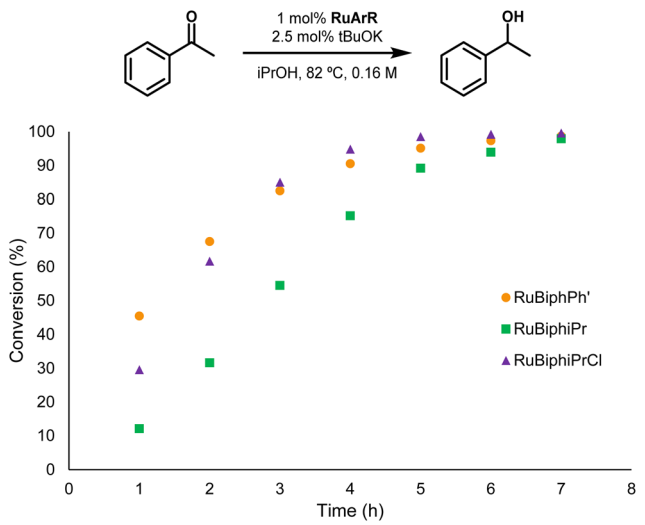

Fig. 14 Conversion of acetophenone *vs.* time with complexes **RuBiphiPr**, **RuBiphiPrCl**, and **RuBiphPh′**.

The three complexes were found to be effective catalysts in the reaction with complexes **RuBiphPh′** and **RuBiphiPrCl** being equally active furnishing over 90% conversion after 4 h, while **RuBiphiPr** is somewhat less active. The activity of the complexes is similar to the previously reported neutral complexes of the type [Ru(η^6-*p*-cymene)Cl_2(**P***)] (**P*** = *P*-stereogenic monophosphane, including **BiphMe**[26–28,93–95]) but in contrast to the moderate enantioselectivity obtained with some of the reported complexes with monophosphanes,[28] the enantioselectivity obtained with the complexes of Fig. 14 was very low (ee < 10%).

Conclusions

In this paper the rich coordination chemistry towards Rh(I) and Ru(II) of a group of six *P*-stereogenic, methylene-bridged, unsymmetrical diphosphanes has been studied. Two out of these six ligands, bearing two *tert*-butyl moieties on the non-*P*-stereogenic phosphorus, are described for the first time in this paper.

For Rh, mono(chelated) and bis(chelated) structures have been synthesized and isolated. The bis(chelated) complexes present the *cis*- and the *trans*-isomers, and it has been observed that the former crystallizes preferentially, which has allowed us to obtain its crystal structure by X-ray diffraction. This selectivity is in accordance with the previous results of the group when coordinating the same ligand to Pd.

For Ru, two different structures have been obtained for the **BiphR** ligands, namely a chelated (κ^2-P^1,P^2), and a monocoordinated (κ^1-P^2) one, the latter with the ligand coordinated through the non-*P*-stereogenic phosphorus atom. The ligand **BiphiPr** shows a preference for the chelated structure, while **BiphPh** also forms the monocoordinated and the chelated complexes. The clean formation of the monocoordinated complex is very interesting, since it is an obvious entryway to heterobimetallic complexes with a variety of methylene-bridged diphosphanes, which up to now have only been studied with parent dppm, but already showing promising biological activities, especially the Ru(II)–Au(I) and Ru(II)–Fe(II) complexes.[64,77,96–98]

Lastly, the applicability of the different complex structures has been tested in asymmetric catalysis. For the Rh complexes, asymmetric hydrogenation has been studied, while for the Ru ones the chosen reaction has been asymmetric transfer hydrogenation. The conversion has been excellent in both cases, although the enantioselectivity has ranged between moderate and low.

Experimental part

Generalities

All compounds were prepared under a purified nitrogen atmosphere using standard Schlenk and vacuum-line techniques or inside a glovebox. The solvents were purified by a solvent puri-

fication system or by standard procedures[99] and kept under nitrogen. ^{1}H, ^{13}C{^{1}H}, ^{31}P{^{1}H}, and bidimensional NMR spectra were recorded at room temperature with 400 or 500 MHz spectrometers. The fields are 400 or 500 MHz (^{1}H), 101 or 126 MHz (^{13}C{^{1}H}) and 162 or 202 MHz (^{31}P{^{1}H}). Chemical shifts are reported downfield from standards ($SiMe_4$ for ^{1}H and ^{13}C and H_3PO_4 for ^{31}P NMR) and the coupling constants are given in Hz. IR spectra were recorded with an ATR and the main absorption bands are expressed in cm^{-1}. High-resolution mass analyses (HRMS) were carried out in a time-of-flight instrument using electrospray ionisation. Diphosphanes **BiphiPr**, **NpiPr**, **BiphPh** and **NpPh** were prepared following the reported procedure.[29]

Ligands

Biph*t*Bu. (*S*)-(2-Biphenylyl)(methyl)(phenyl)phosphane–borane (**BiphMe**, 290 mg, 1.0 mmol) was dissolved in 5 mL of THF and the solution was cooled to −78 °C. *s*-BuLi (1.0 mL of a 1.3 M solution, 1.3 mmol) was added and the solution was stirred for 2 h. The solution was then cooled to −78 °C and chloroditertbutylphosphane (220 μL, 1.1 mmol) was added, allowing the mixture reach room temperature while stirring overnight.

The next day, 1 mL of methanol was added, and the mixture was brought to dryness. After that, it was dissolved in 5 mL of morpholine and stirred for 24 h at room temperature. The solvent was evaporated *in vacuo*, and the residue was subjected to column chromatography purification (alumina, toluene) under nitrogen to yield the desired product as a viscous white oil. Yield: 90% (379 mg).

^{1}H NMR (400 MHz, C_6D_6): 7.48–7.41 (m, 1H, Ar), 7.37–7.28 (m, 2H, Ar), 7.26–7.19 (m, 2H, Ar), 7.10–6.79 (m, 9H, Ar), 1.89–1.81 (m, 2H, $CH_{2(bridge)}$), 0.84 (d, J = 10.8, 9H, $CH_{3(tBu)}$), 0.76 (d, J = 10.5, 9H, $CH_{3(tBu)}$). **^{13}C{^{1}H} NMR (101 MHz, C_6D_6):** 147.8–122.1 (m, 18C, Ar), 30.7 (m, 2C, C_{tBu}), 28.7 (m, 6C, $CH_{3(tBu)}$), 20.1 (dd, J = 36.1, 24.1, 1C, $CH_{2(bridge)}$). **^{31}P{^{1}H} NMR (162 MHz, C_6D_6):** +13.8 (d, J = 129.8, P^2), −25.1 (d, J = 129.8, P^1).

Np*t*Bu. This compound was prepared analogously to **Biph*t*Bu** with (*S*)-(1-naphthyl)(methyl)(phenyl)phosphane–borane (**NpMe**). Yield: 87% (343 mg).

^{1}H NMR (400 MHz, C_6D_6): 8.66 (m, 1H, Ar), 7.64 (ddd, J = 7.1, 4.1, 1.3, 1H, Ar), 7.49–7.36 (m, 3H, Ar), 7.20–7.10 (m, 1H, Ar), 7.07–6.87 (m, 3H, Ar), 6.88–6.78 (m, 3H, Ar), 2.36–2.28 (m, 1H, CH_{bridge}), 2.06–1.96 (m, 1H, CH_{bridge}), 0.93 (d, J = 10.8, 9H, $CH_{3(tBu)}$), 0.80 (d, J = 10.8, 9H, $CH_{3(tBu)}$). **^{13}C{^{1}H} NMR (101 MHz, C_6D_6):** 133.3–123.1 (m, 16C, Ar), 30.8 (m, 2C, C_{tBu}), 29.6–27.8 (m, 6C, $CH_{3(tBu)}$), 20.6–18.7 (m, 1C, $CH_{2(bridge)}$). **^{31}P{^{1}H} NMR (162 MHz, C_6D_6):** +13.8 (d, $^{2}J_{P^1-P^2}$ = 144.0, P^2), −28.1 (d, $^{2}J_{P^1-P^2}$ = 144.0, P^1).

Rhodium complexes

RhBiphiPr. Diphosphane **BiphiPr** (84.4 mg, 0.22 mmol) was dissolved in 10 mL of CH_2Cl_2 and added dropwise during 30 min to a solution of $[Rh(COD)_2]BF_4$ (82 mg, 0.20 mmol) in 5 mL of CH_2Cl_2. The resulting solution was left stirring for 1 h and the solvent was evaporated *in vacuo*. The obtained orange solid was recrystallized with 2 mL of CH_2Cl_2 and 15 mL of Et_2O and filtered through a Schlenk filter. The final product was transferred to a 5 mL scintillation vial and stored in the freezer inside a glovebox. Yield 33% (45 mg).

^{1}H NMR (400 MHz, CD_2Cl_2): 9.22–9.10 (m, 1H, Ar), 8.52–8.32 (m, 3H, Ar), 8.31–8.01 (m, 5H, Ar), 7.98–7.85 (m, 4H, Ar), 7.60–7.52 (m, 1H, Ar), 6.46 (s, br, 1H, CH_{COD}), 6.21 (s, br, 1H, CH_{COD}), 5.91 (s, br, 1H, CH_{COD}), 5.67 (s, br, 1H, CH_{COD}), 4.41–4.29 (m, 1H, CH_{bridge}), 3.98–3.86 (m, 1H, CH_{bridge}), 3.39–3.08 (m, 8H, $CH_{2(COD)}$), 3.07–2.96 (m, 1H, CH_{iPr}), 2.89–2.80 (m, 1H, CH_{iPr}), 2.12 (dd, J = 17.8, 7.2, 3H, $CH_{3(iPr)}$), 2.00–1.74 (m, 6H, $CH_{3(iPr)}$). **^{13}C{^{1}H} NMR (101 MHz, CD_2Cl_2):** 142.2–123.3 (m, 18C, CH_{Ar}), 99.5 (s, 1C, CH_{COD}), 95.0 (s, 1C, CH_{COD}), 93.8 (s, 1C, CH_{COD}), 93.6 (s, 1C, CH_{COD}), 27.8 (dd, J = 24.6, 19.0, 1C, $CH_{2(bridge)}$), 26.5–24.7 (m, 4C, $CH_{2(COD)}$), 21.2–20.4 (m, 2C, CH_{iPr}), 14.6 (s, 1C, $CH_{3(iPr)}$), 14.0 (s, 1C, $CH_{3(iPr)}$), 13.8 (s, 1C, $CH_{3(iPr)}$), 12.6 (s, 1C, $CH_{3(iPr)}$). **^{31}P{^{1}H} NMR (202 MHz, CD_2Cl_2):** −13.4 (dd, $^{1}J_{P^2-Rh}$ = 126.9, $^{2}J_{P^1-P^2}$ = 76.1, P^2), −34.9 (dd, $^{1}J_{P^1-Rh}$ = 129.4, $^{2}J_{P^1-P^2}$ = 76.1, P^1). **HRMS:** calcd for $[M - BF_4 + 2O]^+$ 635.1715, found 635.1703. **IR:** 2962, 1629, 1435, 1258, 1037, 879, 795, 702.

RhBiph*t*Bu. The same method used for **RhBiphiPr** was followed. The starting diphosphane was **Biph*t*Bu** (95 mg, 0.23 mmol). Yield 64% (92 mg).

^{1}H NMR (400 MHz, CD_2Cl_2): 7.63–7.56 (m, 2H, Ar), 7.47–7.14 (m, 6H, Ar), 7.04–7.01 (m, 2H, Ar), 6.96–6.91 (m, 2H, Ar), 6.59–6.57 (m, 2H, Ar), 5.91 (s, br, 1H, CH_{COD}), 5.49 (s, br, 1H, CH_{COD}), 4.86 (s, br, 1H, CH_{COD}), 4.64 (s, br, 1H, CH_{COD}), 3.56–3.42 (m, 1H, CH_{bridge}), 3.21–3.07 (m, 1H, CH_{bridge}), 2.61–1.98 (m, 8H, $CH_{2(COD)}$), 1.30 (d, J = 14.5, 9H, $CH_{3(tBu)}$), 1.11 (d, J = 14.8, 9H, $CH_{3(tBu)}$). **^{13}C{^{1}H} NMR (101 MHz, CD_2Cl_2):** 146.7–126.2 (m, 18C, CH_{Ar}), 103.4–103.0 (m, 1C, CH_{COD}), 101.5–101.0 (m, 1C, CH_{COD}), 99.3–98.9 (m, 1C, CH_{COD}), 91.7–91.3 (m, 1C, CH_{COD}), 37.1 (dd, J = 7.5, 3.6, 1C, $C_{(tBu)}$), 36.0 (d, J = 7.2, 1C, $C_{(tBu)}$), 33.3 (dd, J = 23.6, 13.7, 1C, $CH_{2(bridge)}$), 31.5 (s, 1C, $CH_{2(COD)}$), 30.7 (s, 1C, $CH_{2(COD)}$), 29.4 (d, J = 4.9, 3C, $CH_{3(tBu)}$), 29.3 (d, J = 5.6, 3C, $CH_{3(tBu)}$), 29.1 (s, 1C, $CH_{2(COD)}$), 28.9 (s, 1C, $CH_{2(COD)}$). **^{31}P{^{1}H} NMR (202 MHz, CD_2Cl_2):** −4.7 (dd, $^{1}J_{P^2-Rh}$ = 125.4, $^{2}J_{P^1-P^2}$ = 63.1, P^2), −35.8 (dd, $^{1}J_{P^1-Rh}$ = 130.6, $^{2}J_{P^1-P^2}$ = 63.1, P^1). **HRMS:** calcd for $[M - COD - BF_4]^+$ 523.1191, found 523.1183. **IR:** 2951, 2081, 2031, 1466, 1435, 1062, 736, 704.

RhBiphPh. The same method used for **RhBiphiPr** was followed. The starting diphosphane was **BiphPh** (104 mg, 0.23 mmol). Yield 22% (38 mg).

^{1}H NMR (400 MHz, CD_2Cl_2): 7.57–7.01 (m, 24H, Ar), 5.22 (s, br, 1H, CH_{COD}), 5.04 (s, br, 2H, CH_{COD}), 4.59 (s, br, 1H, CH_{COD}), 4.08–3.94 (m, 1H, CH_{bridge}), 3.70–3.58 (m, 1H, CH_{bridge}), 2.39–2.07 (m, 8H, $CH_{2(COD)}$). **^{13}C{^{1}H} NMR (101 MHz, CD_2Cl_2):** 146.9–126.3 (m, 30C, CH_{Ar}), 102.8–102.4 (m, 1C, CH_{COD}), 100.3–99.9 (m, 1C, CH_{COD}), 98.3–97.7 (m, 2C, CH_{COD}), 41.1 (t, $^{1}J_{CP}$ = 22.6, 1C, $CH_{2(bridge)}$), 30.8 (s, 1C, $CH_{2(COD)}$), 30.7 (s, 1C, $CH_{2(COD)}$), 29.5 (s, 1C, $CH_{2(COD)}$), 29.0 (s, 1C, $CH_{2(COD)}$). **^{31}P{^{1}H} NMR (162 MHz, CD_2Cl_2):** −29.1 (dd, $^{1}J_{P^2-Rh}$ = 126.6, $^{2}J_{P^1-P^2}$ = 75.7, P^2), −29.8 (dd, $^{1}J_{P^1-Rh}$ = 130.6,

$^{2}J_{P^1-P^2}$ = 75.7, P^1). **HRMS**: calcd for $[M - COD - BF_4 + O]^+$ 687.1453, found 687.1453. **IR**: 2886, 2837, 1481, 1433, 1345, 1314, 1281, 1164, 1091, 1032, 995, 863, 829, 784, 742, 692.

RhNpiPr. The same method used for **RhBiphiPr** was followed. The starting diphosphane was **NpiPr** (80 mg, 0.22 mmol). Yield 54% (72 mg).

^{1}H NMR (400 MHz, CD_2Cl_2): 8.43 (ddd, *J* = 16.8, 6.8, 1.2, 1H, Ar), 8.18 (d, *J* = 8.4, 1H, Ar), 8.02 (d, *J* = 8.0, 1H, Ar), 7.76 (d, *J* = 8.4, 1H, Ar), 7.67 (td, *J* = 7.4, 2.0, 1H, Ar), 7.57 (td, *J* = 7.6, 0.8, 1H, Ar), 7.53–7.40 (m, 6H, Ar), 5.75 (s, br, 1H, CH_{COD}), 5.57 (s, br, 1H, CH_{COD}), 5.15 (s, br, 1H, CH_{COD}), 4.92 (s, br, 1H, CH_{COD}), 4.16–4.06 (m, 1H, CH_{bridge}), 3.66–3.60 (m, 1H, CH_{bridge}), 2.54–2.26 (m, 8H, $CH_{2(COD)}$), 2.08–1.97 (m, 2H, CH_{iPr}), 1.55 (dd, *J* = 15.0, 6.9, 3H, $CH_{3(iPr)}$), 1.26 (dd, *J* = 15.0, 6.9, 3H, $CH_{3(iPr)}$), 1.10 (dd, *J* = 17.9, 7.1, 3H, $CH_{3(iPr)}$), 0.83 (dd, *J* = 17.3, 6.9, 3H, $CH_{3(iPr)}$). **^{13}C{^{1}H} NMR (101 MHz, $CDCl_3$)**: 138.0–124.0 (m, 16C, CH_{Ar}), 102.9–102.7 (m, 1C, CH_{COD}), 99.6–99.4 (m, 1C, CH_{COD}), 99.1–99.0 (m, 1C, CH_{COD}), 96.2–96.1 (m, 1C, CH_{COD}), 33.8–33.3 (m, 1C, $CH_{2(bridge)}$), 30.8 (s, 1C, $CH_{2(COD)}$), 30.1 (s, 1C, $CH_{2(COD)}$), 30.0 (s, 1C, $CH_{2(COD)}$), 29.4 (s, 1C, $CH_{2(COD)}$), 25.5–25.2 (m, 2C, $CH_{(iPr)}$), 19.4 (d, *J* = 3.1, 1C, $CH_{3(iPr)}$), 18.3 (s, 1C, $CH_{3(iPr)}$), 18.6 (d, *J* = 4.0, 1C, $CH_{3(iPr)}$), 17.4 (s, 1C, $CH_{3(iPr)}$). **^{31}P{^{1}H} NMR (162 MHz, CD_2Cl_2)**: −12.3 (dd, $^1J_{PRh}$ = 126.7, $^2J_{PP}$ = 77.4, P^2), −39.1 (dd, $^1J_{PRh}$ = 131.7, $^2J_{PP}$ = 77.4, P^1). **HRMS**: calcd for $[M - COD - BF_4 + 2CH_3CN]^+$ 567.1201, found 567.1206. **IR**: 2922, 1696, 1506, 1458, 1436, 1335, 1052, 881, 805, 694, 663, 639.

RhNp*t*Bu. The same method used for **RhBiphiPr** was followed, with the exception that the diphosphane was dissolved in 20 mL of CH_2Cl_2 and added over 2 h. The starting diphosphane was **Np*t*Bu** (78.9 mg, 0.2 mmol). Yield 42% (92 mg, 0.126 mmol).

^{1}H NMR (500 MHz, CD_2Cl_2): 8.69 (ddd, *J* = 17.2, 7.0, 1.3, 1H, Ar), 8.20 (d, *J* = 8.5, 1H, Ar), 8.02 (d, *J* = 8.0, 1H, Ar), 7.98 (d, *J* = 8.0, 1H, Ar), 7.73–7.34 (m, 8H, Ar), 6.07 (s, br, 1H, CH_{COD}), 5.74 (s, br, 1H, CH_{COD}), 4.98 (s, br, 1H, CH_{COD}), 4.68 (s, br, 1H, CH_{COD}), 4.25 (ddd, *J* = 16.7, 10.8, 8.3, 1H, CH_{bridge}), 3.79–3.68 (m, 1H, CH_{bridge}), 2.70–2.60 (m, 2H, $CH_{2(COD)}$), 2.57–2.46 (m, 1H, $CH_{2(COD)}$), 2.35 (m, 2H, $CH_{2(COD)}$), 2.28–2.18 (m, 3H, $CH_{2(COD)}$), 1.59 (d, *J* = 14.5, 9H, $CH_{3(tBu)}$), 1.07 (d, *J* = 14.9, 9H, $CH_{3(tBu)}$). **^{13}C{^{1}H} NMR (126 MHz, CD_2Cl_2)**: 142.2–121.8 (m, 16C, Ar), 104.2 (s, 1C, CH_{COD}), 101.3 (s, 1C, CH_{COD}), 94.5 (s, 1C, CH_{COD}), 91.5 (s, 1C, CH_{COD}), 36.2 (m, 1C, $CH_{2(bridge)}$), 31.7 (s, 1C, $CH_{2(COD)}$), 31.2 (s, 1C, $CH_{2(COD)}$), 30.0 (d, *J* = 5.1, $CH_{3(tBu)}$), 29.7 (d, *J* = 6.0, $CH_{3(tBu)}$), 29.4 (s, 1C, C_{tBu}), 29.3 (s, 1C, C_{tBu}). **^{31}P{^{1}H} NMR (202 MHz, CD_2Cl_2)**: −2.9 (dd, $^1J_{P^2-Rh}$ = 125.1, $^2J_{P^1-P^2}$ = 63.9, P^2), −38.3 (dd, $^1J_{P^1-Rh}$ = 132.7, $^2J_{P^1-P^2}$ = 63.9, P^1). **IR**: 2962, 2237, 1588, 1435, 1262, 1047, 886, 804, 775, 731, 694.

RhNpPh. The same method used for **RhBiphiPr** was followed. The starting diphosphane was **NpiPr** (80 mg, 0.22 mmol). Yield 42% (92 mg).

^{1}H NMR (500 MHz, CD_2Cl_2): 8.26 (d, *J* = 8.5, 1H, Ar), 8.05 (d, *J* = 8.0, 1H, Ar), 8.00 (d, *J* = 8.0, 1H, Ar), 7.87 (ddd, *J* = 16.0, 7.0, 1.5, 1H, Ar), 7.62–7.35 (m, 18H, Ar), 5.47 (s, br, 1H, CH_{COD}), 5.32 (s, br, 3H, CH_{COD}), 4.47–4.43 (m, 2H, CH_{bridge}), 2.42–2.21 (m, 8H, $CH_{2(COD)}$). **^{13}C{^{1}H} NMR (126 MHz, CD_2Cl_2)**: 137.5–125.0 (m, Ar), 103.7 (s, CH_{COD}), 101.1 (m, CH_{COD}), 100.1 (s, CH_{COD}), 42.4 (t, *J* = 21.9, 1C, $CH_{2(bridge)}$), 30.5 (m, $CH_{2(COD)}$). **^{31}P{^{1}H} NMR (162 MHz, CD_2Cl_2)**: −28.9 (dd, $^1J_{P2-Rh}$ = 130.2, $^2J_{P^1-P^2}$ = 78.0, P^2), −33.1 (dd, $^1J_{P^1-Rh}$ = 130.1, $^2J_{P^1-P^2}$ = 78.0, P^1). **HRMS**: calcd for $[M - COD - BF_4 + 2O]^+$ 677.1246, found 677.1238. **IR**: 2887, 2838, 1482, 1434, 1345, 1314, 1282, 1165, 1090, 1050, 992, 864, 828, 804, 776, 741, 962.

Rh(BiphiPr)$_2$. $Rh[COD_2]BF_4$ (235 mg, 0.3 mmol) was dissolved in 5 mL of CH_2Cl_2 and added to a CH_2Cl_2 solution of the same volume containing the free diphosphane **BiphiPr** (123 mg, 0.6 mmol). The mixture was stirred for 1 h and the solvent was evaporated *in vacuo*. The resulting orange residue was recrystallized with 2 mL of CH_2Cl_2 and 15 mL of Et_2O, affording an oil that, after a night in the freezer, precipitated into a solid. Yield 21% (62 mg).

^{1}H NMR (500 MHz, CD_2Cl_2): 7.71–6.50 (m, 28H, Ar), 3.39–3.18 (m, 2H, CH_{bridge}), 2.77–2.64 (m, 2H, CH_{bridge}), 1.98–1.90 (m, 1H, CH_{iPr}), 1.82–1.72 (m, 3H, CH_{iPr}), 1.27–0.63 (m, 24H, $CH_{3(iPr)}$). **^{13}C{^{1}H} NMR (126 MHz, CD_2Cl_2)**: 132.9–126.2 (m, Ar), 33.9 (m, $CH_{2(bridge)}$), 25.7 (m, CH_{iPr}), 24.9 (m, CH_{iPr}), 19.5–15.3 (m, $CH_{3(iPr)}$). **^{31}P{^{1}H} NMR (202 MHz, CD_2Cl_2)**: 0.3–(−1.8) (m, P^2_{cis}), −1.8–(−3.9) (m, P^2_{cis}), −6.7–(−9.0) (m, P^2_{trans}), −17.3–(−19.6) (m, P^1_{trans}), −24.2–(−26.1) (m, P^1_{cis}), −26.1–(−28.2) (m, P^1_{cis}). **HRMS**: calcd for $[M - BF_4]^+$ 887.2701, found 887.2698. **IR**: 3054, 2957, 1460, 1438, 1049, 735, 694, 630.

Ruthenium complexes

RuBiphiPr. The precursor $[RuCl(\mu\text{-}Cl)Cl(p\text{-cymene})_2]_2$ (64 mg, 0.1 mmol) and NH_4PF_6 (945 mg, 5.9 mmol) was dissolved in 10 mL of CH_2Cl_2 and **BiphiPr** (98 mg, 0.25 mmol) was added. The solution was stirred for about 1 h at room temperature and, after that, the solvent was evaporated *in vacuo* and recrystallised with CH_2Cl_2 and Et_2O. Yield 90% (150 mg).

^{1}H NMR (400 MHz, $CDCl_3$): 8.10 (ddd, *J* = 17.2, 8.0, 0.8, 1H, Ar), 7.88 (dt, *J* = 8.0, 2.0, 1H, Ar), 7.62 (dt, *J* = 7.2, 1.6, 1H, Ar), 7.40–7.35 (m, 1H, Ar), 7.32–7.24 (m, 5H, Ar), 7.20 (ddd, *J* = 7.6, 4.0, 1.6, 1H, Ar), 7.16–7.12 (m, 2H, Ar), 6.66–6.58 (m, 2H, Ar), 6.26 (d, *J* = 6.1, 1H, $Ar_{(p\text{-cymene})}$), 6.07 (d, *J* = 6.5, 2H, $Ar_{(p\text{-cymene})}$), 5.90 (d, *J* = 6.1, 1H, $Ar_{(p\text{-cymene})}$), 5.73 (d, *J* = 6.4, 1H, $Ar_{(p\text{-cymene})}$), 3.57–3.42 (m, 1H, CH_{bridge}), 3.42–3.27 (m, 1H, CH_{bridge}), 2.76–2.62 (m, 1H, CH_{iPr}), 2.62–2.52 (m, 1H, $CH_{i_{Pr}(p\text{-cymene})}$), 2.35–2.22 (m, 1H, CH_{iPr}), 2.10 (s, 3H, $CH_{3(p\text{-cymene})}$), 1.30 (dd, *J* = 7.2, 2.6, 3H, $CH_{3(iPr)}$), 1.26 (dd, *J* = 7.3, 2.0, 3H, $CH_{3(iPr)}$), 1.22 (d, *J* = 7.3, 3H, $CH_{3(iPr,\ p\text{-cymene})}$), 1.03 (dd, *J* = 13.9, 6.9, 6H, $CH_{3(iPr)}$), 0.96 (dd, *J* = 15.7, 7.2, 3H, $CH_{3(iPr)}$). **^{13}C{^{1}H} NMR (101 MHz, $CDCl_3$)**: 145.1–128.0 (m, 18C, Ar), 120.1 (s, 1C, $Ar_{(p\text{-cymene})}$), 101.8 (s, 1C, $Ar_{(p\text{-cymene})}$), 94.0 (d, *J* = 7.1, 1CH, $Ar_{(p\text{-cymene})}$), 89.6 (d, *J* = 6.0, 1CH, $Ar_{(p\text{-cymene})}$), 89.2 (d, *J* = 6.3, 1CH, $Ar_{(p\text{-cymene})}$), 87.7 (s, 1CH, $Ar_{(p\text{-cymene})}$), 35.0 (dd, *J* = 27.3 21.2, 1C, $CH_{2(bridge)}$), 31.2 (s, 1C, $CH_{i_{Pr}(p\text{-cymene})}$), 27.6 (d, *J* = 21.5, 1C, CH_{iPr}), 26.1 (dd, *J* = 18.4, 9.9, 1C, CH_{iPr}), 21.9 (d, *J* = 43.8, 2C, $CH_{3(iPr,\ p\text{-cymene})}$), 19.6 (s, 3C, $CH_{3(iPr)}$), 19.2 (s, 1C, $CH_{3(iPr)}$), 19.0 (s, 1C, $CH_{3(p\text{-cymene})}$).

$^{31}P\{^{1}H\}$ NMR (162 MHz, $CDCl_3$): +20.9 (d, $^{2}J_{P^1-P^2}$ = 91.0, P^2), −0.2 (d, $^{2}J_{P^1-P^2}$ = 91.0, P^1), −144.2 (hept, $^{1}J_{P-F}$ = 712.8, PF_6). **HRMS:** calcd for $[M - PF_6]^+$ 663.16502, found 633.1643. **IR:** 2966, 2935, 2880, 1462, 1436, 1387, 1096, 1059, 877, 832, 758, 737, 706, 692, 556, 556.

RuBiphiPrCl. The precursor $[RuCl(\mu\text{-}Cl)Cl(p\text{-cymene})_2]_2$ (197 mg, 0.3 mmol) was dissolved in 10 mL of CH_2Cl_2 and **BiphiPr** (235 mg, 0.60 mmol) was added dropwise with a dropping funnel. The solution was stirred for about 5 h at room temperature and, after that, the solvent was evaporated *in vacuo* and recrystallised with CH_2Cl_2 and Et_2O. Yield: 211 mg (50%).

^{1}H NMR (400 MHz, $CDCl_3$): 8.36 (dd, J = 15.6, 7.2, 1H, Ar), 8.11 (t, J = 6.8, 1H, Ar), 7.61 (t, J = 6.0, 1H, Ar), 7.39–7.08 (m, 9H, Ar), 6.65–6.57 (m, 2H, Ar), 6.47 (s, 1H, $Ar_{(p\text{-cymene})}$), 6.43 (s, 1H, $Ar_{(p\text{-cymene})}$), 6.32 (d, J = 6.5, 1H, $Ar_{(p\text{-cymene})}$), 5.77 (d, J = 6.5, 1H, $Ar_{(p\text{-cymene})}$), 3.46 (ddd, J = 15.2, 12.8, 11.6, 1H, CH_{bridge}), 3.30 (ddd, J = 15.3, 10.5, 9.1, 1H, CH_{bridge}), 2.75–2.63 (m, 1H, $CH_{i\text{Pr}}$), 2.65–2.53 (m, 1H, $CH_{i_{Pr}(p\text{-cymene})}$), 2.37 (m, 1H, $CH_{i\text{Pr}}$), 2.20 (s, 3H, $CH_{3(p\text{-cymene})}$), 1.33–1.14 (m, 9H, $CH_{3(i\text{Pr})}$), 1.03 (d, J = 6.1, 6H, $2CH_{3(p\text{-cymene})}$), 0.93 (dd, J = 15.9, 7.2, 3H, $CH_{3(i\text{Pr})}$). **$^{13}C\{^{1}H\}$ NMR (101 MHz, $CDCl_3$):** 144.8–127.9 (m, 18C, Ar), 117.8 (d, 1C, $Ar_{(p\text{-cymene})}$), 102.4 (s, 1C, $C_{p\text{-cymene}}$), 94.4 (d, 1CH, $Ar_{(p\text{-cymene})}$), 90.4 (d, 1CH, $Ar_{(p\text{-cymene})}$), 89.9 (d, 1CH, $Ar_{(p\text{-cymene})}$), 88.6 (s, 1CH, $Ar_{(p\text{-cymene})}$), 34.7 (dd, J_{CP} = 27.1, 20.9, 1C, $CH_{2(bridge)}$), 31.4 (s, 1C, $CH_{(i\text{Pr},\ p\text{-cymene})}$), 27.6 (d, J = 21.3, 1C, $CH_{(i\text{Pr})}$), 26.2 (dd, J = 18.3, 9.9, 1C, $CH_{(i\text{Pr})}$), 22.2 (s, 1C, $CH_{3(i\text{Pr},\ p\text{-cymene})}$), 22.1 (s, 1C, $CH_{3(i\text{Pr},\ p\text{-cymene})}$), 19.8 (s, 1C, $CH_{3(p\text{-cymene})}$), 19.8 (s, 1C, $CH_{3(i\text{Pr})}$), 19.6–19.3 (m, 3C, $CH_{3(i\text{Pr})}$). **$^{31}P\{^{1}H\}$ NMR (162 MHz, $CDCl_3$):** +21.5 (d, $^{2}J_{P^1-P^2}$ = 91.4, P^2), +0.1 (d, $^{2}J_{P^1-P^2}$ = 91.4, P^1). **HRMS:** calcd for $[M - Cl]^+$ 663.1650, found 663.1645. **IR:** 3357, 3051, 2961, 1625, 1459, 1434, 1259, 1090, 1008, 877, 799, 690, 603.

RuBiphPh. RuBiphPh′ (100 mg, 0.13 mmol) was dissolved in 10 mL of DCM, of $TlPF_6$ (52 mg, 0.14 mmol) were added and the solution was vigorously stirred for 48 h. The solution was filtered through a silica pad with Celite® and evaporated to dryness. Yield 44% (59 mg).

^{1}H NMR (400 MHz, $CDCl_3$): 8.36 (dd, J = 17.2, 7.6, 1H, Ar), 7.92 (t, J = 7.6, 1H, Ar), 7.63 (t, J = 6.0, 1H, Ar), 7.42–7.01 (m, 17H, Ar), 7.79 (d, J = 8.4, 1H, Ar), 7.76 (d, J = 7.2, 1H, Ar), 6.58 (d, J = 5.6, 1H, $Ar_{(p\text{-cymene})}$), 6.44–6.42 (m, br, 2H, Ar), 6.17 (d, J = 6.3, 1H, $Ar_{(p\text{-cymene})}$), 5.75 (d, J = 6.3, 1H, $Ar_{(p\text{-cymene})}$), 5.70 (d, J = 5.7, 1H, $Ar_{(p\text{-cymene})}$), 4.06 (dt, J = 15.0, 12.8, 1H, CH_{bridge}), 3.49 (dt, J = 15.2, 10.1, 1H, CH_{bridge}), 2.40–2.26 (m, 1H, $CH_{iPr(p\text{-cymene})}$), 1.37 (s, 3H, $CH_{3(p\text{-cymene})}$), 0.95 (dd, J = 7.1, 2.3, 6H, $CH_{3(iPr,\ p\text{-cymene})}$). **$^{13}C\{^{1}H\}$ NMR (101 MHz, $CDCl_3$):** 143.8–123.3 (m, 30C, Ar), 117.3 (s, 1C, $Ar_{p\text{-cymene}}$), 101.5 (s, 1C, $Ar_{p\text{-cymene}}$), 95.4 (d, 1C, $Ar_{(p\text{-cymene})}$), 89.8 (d, 1C, $Ar_{(p\text{-cymene})}$), 89.3 (d, 1C, $Ar_{(p\text{-cymene})}$), 87.3 (s, 1C, $Ar_{(p\text{-cymene})}$), 39.5 (t, J = 27.3, 1C, $CH_{2(bridge)}$), 30.0 (s, 1C, $CH_{3(p\text{-cymene})}$), 22.0 (s, 1C, $CH_{iPr(p\text{-cymene})}$), 19.7 (s, 1C, $CH_{3(p\text{-cymene})}$), 16.8 (s, 1C, $CH_{3(p\text{-cymene})}$). **$^{31}P\{^{1}H\}$ NMR (162 MHz, $CDCl_3$):** +6.5 (d, $^{2}J_{P^1-P^2}$ = 98.6, P^2), −2.8 (d, $^{2}J_{P^1-P^2}$ = 98.6, P^1), −144.12 (hept, $^{1}J_{PF}$ = 713.0, PF_6). **HRMS:** calcd for $[M - PF_6]^+$ 731.1337, found 731.1326. **IR:** 3057, 2966, 1436, 1302, 1098, 1058, 911, 832, 723, 690, 556.

RuBiphPh′. The same method used for **RuBiphiPr** was followed. The starting diphosphane was **BiphPh** (122 mg, 0.25 mmol). Yield 123 mg (84%).

^{1}H NMR (400 MHz, $CDCl_3$): 7.80–7.71 (m, 2H, Ar), 7.59–7.45 (m, 2H, Ar), 7.38–7.15 (m, 12H, Ar), 7.09–6.95 (m, 4H, Ar), 6.94–6.81 (m, 4H, Ar), 5.28 (d, J = 6.2, 1H, $Ar_{(p\text{-cymene})}$), 5.16 (d, J = 5.8, 2H, $Ar_{(p\text{-cymene})}$), 4.93 (d, J = 6.0, 1H, $Ar_{(p\text{-cymene})}$), 3.52 (dd, J = 16.4, 8.4, 1H, CH_{bridge}), 3.13 (dd, J = 16.0, 8.8, 1H, CH_{bridge}), 2.45 (hept, J = 7.2, 1H, $CH_{iPr(p\text{-cymene})}$), 1.82 (s, 3H, $CH_{3(p\text{-cymene})}$), 0.87 (d, J = 6.8, 3H, $CH_{3(iPr,\ p\text{-cymene})}$), 0.70 (d, J = 6.9, 3H, $CH_{3(iPr,\ p\text{-cymene})}$). **$^{13}C\{^{1}H\}$ NMR (126 MHz, $CDCl_3$):** 135.1–124.4 (m, Ar), 106.8 (s, $Ar_{(p\text{-cymene})}$), 93.9–79.1 (m, $Ar_{(p\text{-cymene})}$), 28.9 (s, $CH_{iPr(p\text{-cymene})}$), 22.6 (s, $CH_{3(p\text{-cymene})}$), 20.7 (s, $CH_{2(bridge)}$), 19.8 (s, $CH_{3(p\text{-cymene})}$). **$^{31}P\{^{1}H\}$ NMR (162 MHz, $CDCl_3$):** +26.0 (d, $^{2}J_{P^1-P^2}$ = 30.8, P^2), −36.9 (d, $^{2}J_{P^1-P^2}$ = 31.0, P^1). **^{1}H NMR (400 MHz, CD_3OD):** 8.36–6.85 (m, 24H, Ar), 6.53 (d, J = 6.4, 1H, $Ar_{(p\text{-cymene})}$), 6.43 (d, J = 6.4, 1H, $Ar_{(p\text{-cymene})}$), 5.87 (d, J = 6.4, 1H, $Ar_{(p\text{-cymene})}$), 5.79 (d, J = 6.0, 1H, $Ar_{(p\text{-cymene})}$), 4.27 (dt, J = 15.3, 12.8, 1H, CH_{bridge}), 3.93 (dt, J = 15.4, 10.1, 1H, CH_{bridge}), 2.34 (septet, J = 6.7, 1H, $CH_{iPr(p\text{-cymene})}$), 1.42 (s, 3H, $CH_{3(p\text{-cymene})}$), 0.97 (d, J = 7.0, 3H, $CH_{3(iPr,\ p\text{-cymene})}$), 0.76 (d, J = 6.9, 3H, $CH_{3(iPr,\ p\text{-cymene})}$). **$^{13}C\{^{1}H\}$ NMR (101 MHz, CD_3OD):** 146.8–125.3 (m, Ar), 94.8 (d, J = 7.5, $Ar_{(p\text{-cymene})}$), 91.8 (d, J = 6.4, $Ar_{(p\text{-cymene})}$), 89.5 (d, J = 6.5, $Ar_{(p\text{-cymene})}$), 88.9 (s, $Ar_{(p\text{-cymene})}$), 40.7 (t, J = 27.7, $CH_{2(bridge)}$), 30.9 (s, $CH_{iPr(p\text{-cymene})}$), 21.9 (s, $CH_{3(iPr,\ p\text{-cymene})}$), 19.7 (s, $CH_{3(iPr,\ p\text{-cymene})}$), 16.4 (s, $CH_{3(p\text{-cymene})}$). **$^{31}P\{^{1}H\}$ NMR (162 MHz, CD_3OD):** +5.8 (d, $^{2}J_{P^1-P^2}$ = 100.4, P^2), −0.78 (d, $^{2}J_{P^1-P^2}$ = 100.4, P^1). **HRMS:** calcd for $[M + H]^+$ 767.1103, found 767.1097. **IR:** 3057, 2966, 1436, 1302, 1098, 1058, 910, 832, 723, 690, 556.

Catalytic runs

General procedure for the Rh-catalysed hydrogenation. A solution with the required amount of the rhodium complex (1 mol%) and the corresponding substrate (165 μmol) in anhydrous and degassed THF was prepared in a flask under a nitrogen atmosphere in the glovebox. In all cases, the concentration of the substrate in the reaction medium was adjusted to 0.2 M. Once the reaction mixture had been prepared, the glass vessel was placed into a steel reactor. The autoclave was purged three times with H_2 gas (at 10 bar without stirring), and finally, the autoclave was pressurized under 20 bar of H_2. The reaction mixture was stirred at 800 rpm at room temperature for 24 h. The autoclave was then slowly depressurized, and the reaction mixture was filtered through a short pad of SiO_2 into a 5 mL scintillation vial, eluting with EtOAc (3 mL). The resulting solution was concentrated under vacuum, and the conversion was determined by ^{1}H NMR spectroscopy. The enantiomeric excess was determined by GC chromatography on chiral stationary phases. The GC machines used were HP5890 Series II using helium as a carrier gas and with a FID detector. For the analysis of the hydrogenations of MAC, a CP-chirasil-D-Val column (25 m × 0.25 mm × 0.12 μm; 180 °C, isothermal) was used. For the hydrogenations of DMI, a Chiraldex β-DM column (30 m × 0.25 mm × 0.12 μm; 80 °C,

isothermal) was used. The reactions were performed twice to ensure reproducibility.

General procedure for the Ru-catalysed transfer hydrogenation. Transfer hydrogenation reactions of acetophenone were carried out in 100 mL Schlenk flasks and in pairs to improve the reproducibility of the data. Under an inert atmosphere, the Schlenk flask was charged with 0.04 mmol (1%) of ruthenium complexes and 0.20 mmol (5%) of potassium *tert*-butoxide. Both solids are dissolved in 25 mL of isopropanol and the mixture was left stirring for 15 min at reflux (82 °C) to activate the catalyst. At this point, 4.0 mmol of acetophenone were added to start the reaction. At the allotted times, aliquots were extracted and analysed by gas chromatography to study the conversion of the reaction. For the GC analysis, the same chromatograph and column used for DMI were employed, but at 120 °C (isothermal).

Author contributions

J. E.: methodology, formal analysis, investigation, validation, data curation, writing-original draft, visualisation. Y. M. M.: investigation, validation, writing-original draft. J. C. C.: investigation. A. V.-F.: methodology, resources, writing-review & editing, supervision, funding acquisition. A. G.: investigation, validation. D. S.: resources, funding acquisition. M. F.-B.: investigation, formal analysis. A. G.: methodology, resources, writing-original draft, supervision, project administration, funding acquisition.

Conflicts of interest

There are no conflicts of interest to declare.

Acknowledgements

We thank the MICINN (PID2020-115658GB-I00) and AGAUR (2021-SGR-01107) for financial support. Y. M. M. thanks IN2UB for a Master fellowship.

References

1 *Phosphorus(III) Ligands in Homogeneous Catalysis: Design and Synthesis*, ed. P. C. J. Kamer and P. W. N. M. van Leeuwen, Wiley, 2012.
2 *Phosphorus Ligands in Asymmetric Catalysis: Synthesis and Applications*, ed. A. Börner, Wiley-VCH, Weinheim, 2008.
3 *Catalytic Asymmetric Synthesis*, ed. T. Akiyama and I. Ojima, Wiley, Hoboken, NJ, 2022.
4 K. M. Pietrusiewicz and M. Zablocka, *Chem. Rev.*, 1994, **94**, 1375–1411.
5 A. Grabulosa, *P-Stereogenic Ligands in Enantioselective Catalysis*, Royal Society of Chemistry, Cambridge, 2011.
6 L. Horner, H. Siegel and H. Büthe, *Angew. Chem., Int. Ed. Engl.*, 1968, **7**, 942–942.
7 W. S. Knowles and M. J. Sabacky, *Chem. Commun.*, 1968, 1445–1446.
8 W. S. Knowles, M. J. Sabacky and B. D. Vineyard, *J. Chem. Soc., Chem. Commun.*, 1972, 10–11.
9 W. S. Knowles, M. J. Sabacky, B. D. Vineyard and D. J. Weinkauff, *J. Am. Chem. Soc.*, 1975, **97**, 2567–2568.
10 W. S. Knowles, *Angew. Chem., Int. Ed.*, 2002, **41**, 1998–2007.
11 O. I. Kolodiazhnyi, in *Phosphorus Chemistry I: Asymmetric Synthesis and Bioactive Compounds*, ed. J.-L. Montchamp, Springer International Publishing, Cham, 2015, pp. 161–236.
12 M. Dutartre, J. Bayardon and S. Jugé, *Chem. Soc. Rev.*, 2016, **45**, 5771–5794.
13 T. Imamoto, *Chem. Rec.*, 2016, **16**, 2659–2673.
14 X. Ye, L. Peng, X. Bao, C.-H. Tan and H. Wang, *Green Synth. Catal.*, 2021, **2**, 6–18.
15 D. S. Glueck, *Synlett*, 2021, **31**, 875–884.
16 S. M. Mansell, *Dalton Trans.*, 2017, **46**, 15157–15174.
17 Y. Yamanoi and T. Imamoto, *J. Org. Chem.*, 1999, **64**, 2988–2989.
18 I. D. Gridnev, Y. Yamamoi, N. Higashi, H. Tsuruta, M. Yasutake and T. Imamoto, *Adv. Synth. Catal.*, 2001, **343**, 118–136.
19 G. Hoge, H. Wu, W. S. Kissel, D. A. Pflum, D. J. Greene and J. Bao, *J. Am. Chem. Soc.*, 2004, **126**, 5966–5967.
20 M. Revés, C. Ferrer, T. León, S. Doran, P. Etayo, A. Vidal-Ferran, A. Riera and X. Verdaguer, *Angew. Chem., Int. Ed.*, 2010, **49**, 9452–9455.
21 E. Cristóbal-Lecina, P. Etayo, S. Doran, M. Revés, P. Martín-Gago, A. Grabulosa, A. R. Constantino, A. Vidal-Ferran, A. Riera and X. Verdaguer, *Adv. Synth. Catal.*, 2014, **356**, 795–804.
22 A. Cabré, A. Riera and X. Verdaguer, *Acc. Chem. Res.*, 2020, **53**, 676–689.
23 A. Vidal-Ferran, A. Grabulosa, X. Verdaguer and A. Riera, in *Catalytic Asymmetric Synthesis*, ed. T. Akiyama and I. Ojima, Wiley, Hoboken, NJ, 2022, ch. 15, pp. 561–616.
24 A. Grabulosa, G. Muller, J. I. Ordinas, A. Mezzetti, M. A. Maestro, M. Font-Bardia and X. Solans, *Organometallics*, 2005, **24**, 4961–4973.
25 L. Rodríguez, O. Rossell, M. Seco, A. Grabulosa, G. Muller and M. Rocamora, *Organometallics*, 2006, **25**, 1368–1376.
26 R. Aznar, A. Grabulosa, A. Mannu, G. Muller, D. Sainz, V. Moreno, M. Font-Bardia, T. Calvet and J. Lorenzo, *Organometallics*, 2013, **32**, 2344–2362.
27 M. Navarro, D. Vidal, P. Clavero, A. Grabulosa and G. Muller, *Organometallics*, 2015, **34**, 973–994.
28 P. Clavero, A. Grabulosa, M. Rocamora, G. Muller and M. Font-Bardia, *Dalton Trans.*, 2016, **45**, 8513–8531.
29 J. C. Córdoba, A. Vidal-Ferran, M. Font-Bardia and A. Grabulosa, *Organometallics*, 2020, **39**, 2511–2525.
30 I. D. Gridnev, M. Yasutake, N. Higashi and T. Imamoto, *J. Am. Chem. Soc.*, 2001, **123**, 5268–5276.
31 K. V. L. Crépy and T. Imamoto, *Adv. Synth. Catal.*, 2003, **345**, 79–101.

32 H. Fernández-Pérez, S. M. A. Donald, I. J. Munslow, J. Benet-Buchholz, F. Maseras and A. Vidal-Ferran, *Chem. – Eur. J.*, 2010, **16**, 6495–6508.
33 H. Fernández-Pérez, J. Benet-Buchholz and A. Vidal-Ferran, *Chem. – Eur. J.*, 2014, **20**, 15375–15384.
34 S. Chakrabortty, K. Konieczny, B. H. Mueller, A. Spannenberg, P. Kamer and J. G. de Vries, *Catal. Sci. Technol.*, 2022, **12**, 1392–1399.
35 C. Salomon, S. Dal Molin, D. Fortin, Y. Mugnier, R. T. Boere, S. Jugé and P. D. Harvey, *Dalton Trans.*, 2010, **39**, 10068–10075.
36 C. Salomon, D. Fortin, N. Khiri, S. Jugé and P. D. Harvey, *Eur. J. Inorg. Chem.*, 2011, 2597–2609.
37 R. M. Stoop, A. Mezzetti and F. Spindler, *Organometallics*, 1998, **17**, 668–675.
38 S. O. Grim, P. H. Smith, I. J. Colquhoun and W. McFarlane, *Inorg. Chem.*, 1980, **19**, 3195–3198.
39 F. Eisenträger, A. Göthlich, I. Gruber, H. Heiss, C. A. Kiener, C. Krüger, J. Ulrich Notheis, F. Rominger, G. Scherhag, M. Schultz, B. F. Straub, M. A. O. Volland and P. Hofmann, *New J. Chem.*, 2003, **27**, 540–550.
40 P. Etayo and A. Vidal-Ferran, *Chem. Soc. Rev.*, 2013, **42**, 728–754.
41 T. L. Gianetti, R. E. Rodríguez-Lugo, J. R. Harmer, M. Trincado, M. Vogt, G. Santiso-Quinones and H. Grützmacher, *Angew. Chem., Int. Ed.*, 2016, **55**, 15323–15328.
42 V. P. Morgalyuk, T. Y. V. Strelkova, E. E. Nifant'ev and V. K. Brel, *Mendeleev Commun.*, 2016, **26**, 397–398.
43 J. M. Ernsting, C. J. Elsevier, W. G. J. De Lange and K. Timmer, *Magn. Reson. Chem.*, 1991, **29**, S118–S124.
44 J. Browning, G. W. Bushnell, K. R. Dixon and R. W. Hilts, *J. Organomet. Chem.*, 1993, **452**, 205–218.
45 P. Hofmann, C. Meier, W. Hiller, M. Heckel, J. Riede and M. U. Schmidt, *J. Organomet. Chem.*, 1995, **490**, 51–70.
46 M. Manger, J. Wolf, M. Teichert, D. Stalke and H. Werner, *Organometallics*, 1998, **17**, 3210–3221.
47 J. F. Hooper, R. D. Young, I. Pernik, A. S. Weller and M. C. Willis, *Chem. Sci.*, 2013, **4**, 1568–1572.
48 S. K. Murphy, A. Bruch and V. M. Dong, *Chem. Sci.*, 2015, **6**, 174–180.
49 A. J. Martínez-Martínez, N. H. Rees and A. S. Weller, *Angew. Chem., Int. Ed.*, 2019, **58**, 16873–16877.
50 T. Imamoto, Y. Horiuchi, E. Hamanishi, S. Takeshita, K. Tamura, M. Sugiya and K. Yoshida, *Tetrahedron*, 2015, **71**, 6471–6480.
51 H. El-Amouri, A. A. Bahsoun and J. A. Osborn, *Polyhedron*, 1988, **7**, 2035–2038.
52 K. Marat, *Spinworks 4.2.0*, University of Manitoba, 2015.
53 G. Fries, J. Wolf, K. Ilg, B. Walfort, D. Stalke and H. Werner, *Dalton Trans.*, 2004, 1873–1881.
54 P. G. Pringle, E. L. Hazeland, A. Chapman and H. Sparkes, *Chem. Commun.*, 2015, **51**, 10206–10209.
55 A. L. Colebatch, A. I. McKay, N. A. Beattie, S. A. Macgregor and A. S. Weller, *Eur. J. Inorg. Chem.*, 2017, 4533–4540.
56 Y. Sawatsugawa, K. Tamura, N. Sano and T. Imamoto, *Org. Lett.*, 2019, **21**, 8874–8878.
57 A. F. M. J. Van Der Ploeg and G. Van Koten, *Inorg. Chim. Acta*, 1981, **51**, 225–239.
58 R. Fornika, C. Six, H. Görls, M. Kessler, C. Krüger and W. Leitner, *Can. J. Chem.*, 2001, **79**, 642–648.
59 J. Tellez, A. Gallen, J. Ferrer, F. J. Lahoz, P. Garcia-Orduna, A. Riera, X. Verdaguer, D. Carmona and A. Grabulosa, *Dalton Trans.*, 2017, **46**, 15865–15874.
60 S. B. Jensen, S. J. Rodger and M. D. Spicer, *J. Organomet. Chem.*, 1998, **556**, 151–158.
61 A. C. Marr, M. Nieuwenhuyzen, C. L. Pollock and G. C. Saunders, *Organometallics*, 2007, **26**, 2659–2671.
62 C. Daguenet, R. Scopelliti and P. J. Dyson, *Organometallics*, 2004, **23**, 4849–4857.
63 N. Aldeghi, D. Romano, C. Marschner, S. Biswas, S. Chakraborty, S. Prince, S. Ngubane and B. Blom, *J. Organomet. Chem.*, 2020, **916**, 121214.
64 A. Benamrane, B. Herry, V. Vieru, S. Chakraborty, S. Biswas, S. Prince, C. Marschner and B. Blom, *J. Organomet. Chem.*, 2021, **934**, 121659.
65 P. E. Garrou, *Chem. Rev.*, 1981, **81**, 229–266.
66 L. J. Hounjet, M. Bierenstiel, M. J. Ferguson, R. McDonald and M. Cowie, *Inorg. Chem.*, 2010, **49**, 4288–4300.
67 O. A. Lenis-Rojas, M. P. Robalo, A. I. Tomaz, A. R. Fernandes, C. Roma-Rodrigues, R. G. Teixeira, F. Marques, M. Folgueira, J. Yáñez, A. A. Gonzalez, M. Salamini-Montemurri, D. Pech-Puch, D. Vázquez-García, M. L. Torres, A. Fernández and J. J. Fernández, *Inorg. Chem.*, 2021, **60**, 2914–2930.
68 D. K. Gupta, A. N. Sahay, D. S. Pandey, N. K. Jha, P. Sharma, G. Espinosa, A. Cabrera, M. C. Puerta and P. Valerga, *J. Organomet. Chem.*, 1998, **568**, 13–20.
69 A. B. Chaplin, R. Scopelliti and P. J. Dyson, *Eur. J. Inorg. Chem.*, 2005, 4762–4774.
70 P. Chuklin, V. Chalermpanaphan, T. Nhukeaw, S. Saithong, K. Chainok, S. Phongpaichit, A. Ratanaphan and N. Leesakul, *J. Organomet. Chem.*, 2017, **846**, 242–250.
71 A. B. Chaplin, C. Fellay, G. Laurenczy and P. J. Dyson, *Organometallics*, 2006, **26**, 586–593.
72 J. Ruiz, M. P. Gonzalo, M. Vivanco, R. Quesada and M. E. G. Mosquera, *Dalton Trans.*, 2009, 9280–9290.
73 L. Rafols, D. Josa, D. Aguilà, L. A. Barrios, O. Roubeau, J. Cirera, V. Soto-Cerrato, R. Pérez-Tomás, M. Martínez, A. Grabulosa and P. Gamez, *Inorg. Chem.*, 2021, **60**, 7974–7990.
74 A. W. Coleman, D. F. Jones, P. H. Dixneuf, C. Brisson, J. J. Bonnet and G. Lavigne, *Inorg. Chem.*, 1984, **23**, 952–956.
75 A. W. Coleman, H. Zhang, S. G. Bott, J. L. Atwood and P. H. Dixneuf, *J. Coord. Chem.*, 1987, **16**, 9–17.
76 F. Estevan, P. Lahuerta, J. Latorre, A. Sanchez and C. Sieiro, *Polyhedron*, 1987, **6**, 473–478.
77 B. Herry, L. K. Batchelor, B. Roufosse, D. Romano, J. Baumgartner, M. Borzova, T. Reifenstahl, T. Collins, A. Benamrane, J. Weggelaar, M. C. Correia, P. J. Dyson and B. Blom, *J. Organomet. Chem.*, 2019, **901**, 120934.

78 J. Popp, S. Hanf and E. Hey-Hawkins, *ACS Omega*, 2020, **4**, 22540–22548.
79 G. R. M. Dowson, M. F. Haddow, J. Lee, R. L. Wingad and D. F. Wass, *Angew. Chem., Int. Ed.*, 2013, **52**, 9005–9008.
80 P. Dierkes and P. W. N. M. van Leeuwen, *J. Chem. Soc., Dalton Trans.*, 1999, 1519–1530.
81 P. W. N. M. van Leeuwen, P. C. J. Kamer, J. N. H. Reek and P. Dierkes, *Chem. Rev.*, 2000, **100**, 2741–2769.
82 R. S. Cahn, C. Ingold and V. Prelog, *Angew. Chem., Int. Ed. Engl.*, 1966, **5**, 385–415.
83 V. Prelog and G. Helmchen, *Angew. Chem., Int. Ed. Engl.*, 1982, **21**, 567–583.
84 C. Lecomte, Y. Dusausoy, J. Protas, J. Tirouflet and A. Dormond, *J. Organomet. Chem.*, 1974, **73**, 67–76.
85 The different absolute configurations of the products stems from the Cahn–Ingold–Prelog priority rules.
86 In the two crystal structures the most relevant distances and angles are very similar. Selected parameters in **RhBiph*t*Bu** *vs.* [Rh(COD)TCFP]BF_4: Rh–P1 (2.2861(7) *vs.* 2.2867(18); Rh–P2 (2.3356(7) *vs.* 2.3377(18); P1–Rh–P2 (72.35(2) *vs.* 72.55(6).
87 H. Clavier and S. P. Nolan, *Chem. Commun.*, 2010, **46**, 841–861.
88 A. Poater, B. Cosenza, A. Correa, S. Giudice, F. Ragone, V. Scarano and L. Cavallo, *Eur. J. Inorg. Chem.*, 2009, 1759–1766.
89 L. Falivene, R. Credendino, A. Poater, A. Petta, L. Serra, R. Oliva, V. Scarano and L. Cavallo, *Organometallics*, 2016, **35**, 2286–2293.
90 L. Falivene, Z. Cao, A. Petta, L. Serra, A. Poater, R. Oliva, V. Scarano and L. Cavallo, *Nat. Chem.*, 2019, **11**, 872–879.
91 The absolute configurations of the stereogenic phosphorus are different in the crystal structures (*S* for **Biph*t*Bu** and *R* for TCFP, as free ligands) and for this reason the unhindered quadrants are different in the two steric maps of Fig. 13.
92 P. Rojo, A. Riera and X. Verdaguer, *Org. Lett.*, 2021, **23**, 4802–4806.
93 A. Grabulosa, A. Mannu, A. Mezzetti and G. Muller, *J. Organomet. Chem.*, 2012, **696**, 4221–4228.
94 P. Clavero, A. Grabulosa, M. Font-Bardia and G. Muller, *J. Mol. Catal. A: Chem.*, 2014, **391**, 183–190.
95 J. Popp, A.-M. Caminade and E. Hey-Hawkins, *Eur. J. Inorg. Chem.*, 2020, 1654–1669.
96 L. Massai, J. Fernandez-Gallardo, A. Guerri, A. Arcangeli, S. Pillozzi, M. Contel and L. Messori, *Dalton Trans.*, 2015, **44**, 11067–11076.
97 J. Fernández-Gallardo, B. T. Elie, M. Sanaú and M. Contel, *Chem. Commun.*, 2016, **52**, 3155–3158.
98 B. T. Elie, Y. Pechenyy, F. Uddin and M. Contel, *JBIC, J. Biol. Inorg. Chem.*, 2018, **23**, 399–411.
99 W. L. F. Armarego, *Purification of Laboratory Chemicals*, Butterworth Heinemann, Oxford, Eight edn., 2017.